TÉCNICO LISBOA

Behaviour of a Façade Anchor System under Simulated Seismic Action

Inês Roque Domingues

Thesis to obtain the Master of Science Degree in

Civil Engineering

Supervisors:

Prof. Luís Manuel Coelho Guerreiro

Prof. Giovanni Muciaccia

Examination Committee

Chairperson: Prof. António Manuel Figueiredo Pinto da Costa

Supervisor: Prof. Luís Manuel Coelho Guerreiro

Member of the Committee: Prof. Jorge Miguel Silveira Filipe Mascarenhas Proença

November 2017

Acknowledgements

First and foremost, I would like to express my sincere gratitude to SPIT for allowing access to the data used on this research. This thesis would not be viable without their contribution together with *Laboratorio Prove Materiali, Strutture e Costruzione (LPMSC)* at Politecnico di Milano and *Centre Scientifique et Technique du Bâtiment* that performed all the test protocols included in this study.

Furthermore, this work would not be possible without my thesis supervisors: Professor Giovanni Muciaccia, from Politecnico di Milano, that presented me with this opportunity and accepted to guide me even through the distance obstacle and Professor Luís Guerreiro, from Instituto Superior Técnico, that accepted this project and whose door was always open. I would like to express my gratitude for their contribution and availability, that were crucial for this thesis. I would also like to thank Giuseppe Di Nunzio that followed and helped with every step of this analysis.

Moreover, I am deeply grateful to my parents for all the opportunities and support, and specially for encouraging me to go further and for never doubting me. To my brother, Catarina, Constança, Inês, João, Margarida, Mariana and Raquel for their friendship and motivation bust when needed and to Ahmed, Cristian, Doruk, Hanna, Idil and Mustafa for making Milan my second home. A special mention to Bernardo for embarking on this adventure with me.

Resumo

Nos últimos anos a segurança sísmica de estruturas sofreu uma evolução significativa. Contudo, apesar da minimização da perda de vidas humanas devido a colapsos estruturais, os danos em elementos não-estruturais continuam a ser um tópico relevante devido ao seu impacto social e económico, em especial em edifícios críticos. O projecto destes elementos é baseado nas suas forças de inércia, sendo a sua segurança dependente do dimensionamento correcto dos sistemas de fixação ao elemento portante. Consequentemente, é essencial um dimensionamento seguro desta ligação para as acções esperadas durante um evento sísmico.

O estudo de um sistema de fachada é realizado, utilizando dados provenientes de testes experimentais em parafusos isolados e numa parede à escala real, permitindo uma análise do comportamento do sistema solicitado pela simulação de uma carga dinâmica. Os testes experimentais consistem em deslocamentos impostos no plano da fachada onde é esperada a maior amplificação da aceleração do sistema.

Tendo como base uma análise dinâmica simplificada, é feita uma comparação entre os dados experimentais e prescrições de códigos europeus. É possível mostrar que um coeficiente de comportamento de 1.5 pode ser mais apropriado para solicitações perto da ressonância. Adicionalmente, um estudo sobre o comportamento de um grupo de fixações é realizado, permitindo a conclusão de que 50% poderá ser uma estimativa razoável para a redistribuição de forças entre dois parafusos, cuja rigidez relativa representa um rácio acima de 65%. É provado que a redistribuição de forças, para uma vibração no próprio plano, não afecta a frequência natural da estrutura.

Palavras-Chave

Elementos Não-Estruturais, Sistemas de Fixação, Acção Sísmica, Sistemas de Painéis de Fachada, Análise Dinâmica.

Abstract

In the past years a lot of improvement has been made on earthquake safety of buildings, however, although the loss of life has been minimized due to structural collapses, damage of non-structural elements is still an important topic. Such damage has major social or economical impact, particularly in critical buildings. Being the safety of these elements under seismic load attained by designing them for the forces transferred due to the element's inertia, safety depends on the proper anchoring into the structural element. Hence, it is essential to safely design the connection for the expected actions during an earthquake event.

Thus, the analysis of a façade cladding system is done using data stemming from tests performed on both single fasteners and on a test frame allowing an investigation of the behaviour of the system under a simulated dynamic load. This analysis is made for inplane movement which is expected to be the higher amplified vibration mode.

Under a simplified dynamic analysis, a comparison between experimental data and code prescriptions is attained. It is shown that a behaviour factor of 1.5 may be more suitable for close to resonance states. Moreover, a study of the behaviour of anchors working in a group is made, allowing the conclusion that 50% of forces' redistribution is a reasonable estimation, for two fasteners with a stiffness ratio over 65%. It is also shown that for inplane vibration this redistribution may be negligible on the systems natural frequency.

Key Words

Non-Structural Element, Post-installed Anchors, Seismic Load, Façade Cladding System, Dynamic Analysis.

Contents

List of Figures

List of Tables

List of Symbols

Latin Symbols

a	Acceleration
a_g	Ground acceleration
a_p	Component amplification factor
A_a	Seismic amplification factor
c	Damping coefficient
c_{min}	Minimum allowable edge distance
E	Young modulus
f	Frequency
f_1	Natural frequency
f_D	Damping force
f_I	Inertial force
f_S	Elastic force
F	Force
F_a	Horizontal seismic force
F_{Rk}	Characteristic resistance
g	Gravity acceleration
h_t	Average roof height of the building with respect to the base
H	Total height of the building
$H(f)$	Frequency response function
I	Inertia
I_p	Importance Factor
k	Stiffness
k_b	Bracket stiffness
k_L	Axial stiffness
k_φ	Rotational stiffness
k_{res}	Residual stiffness
K_{alea}	Load distribution coefficient
m	Mass

M_r	Resisting moment
N	Normal force
N_{Sd}	Design value of normal force
N_{Rk}	Characteristic anchor axial resistance
p	Dynamic load
q_a	Behaviour factor
R_a	Support Reaction coefficient
R_p	Response modification factor
S	Soil factor
S_{DS}	Spectral acceleration at short period structures
S_{MS}	Mapped considered earthquake spectral response acceleration for short periods
t	Time
T_1	Fundamental period
v	Position
$\dot{v}$	Velocity
$\ddot{v}$	Acceleration
V_{Rk}	Characteristic anchor shear resistance
W	Weight
z	Height of the point of attachment of component with respect to the base
Z_a	Height of the non-structural element above the base of the building

Greek Symbols

α	Amplification factor
β	Ratio between natural period of the element and natural period of the supporting structure
γ	Importance factor
δ	Logarithmic decrement
Δ	Roof deformation
ζ	Damping ratio
ω	Circular frequency

List of Acronyms

ACI	American Concrete Institute
CEN	European Committee for Standardization
CSTB	Centre Scientifique et Technique du Bâtiment
EC8	Eurocode 8
EOTA	European Organisation for Technical Assessment
ETAG	European Technical Approval Guidelines
FRS	Floor Response Spectrum
IBC	International Building Code
NSEs	Non-Structural Elements
SDOF	Single Degree of Freedom
SEs	Structural Elements

Chapter 1

Introduction

This master dissertation was developed under a double degree program in collaboration between two universities: Politecnico di Milano, in Italy, and Instituto Superior Técnico, in Portugal. It was based on a research project performed in a partnership between Politecnico di Milano and Centre Scientifique et Technique du Bâtiment, which goal was to evaluate the behaviour of plastic anchors for fixing façade claddings through angle brackets, in masonry and concrete, under seismic action.

The purpose of this work is to evaluate not only the behaviour of the anchored systems to structural elements but also the seismic design of this type of non-structural systems. The analysis is supported by several test protocols performed in both research centres that allow a better understanding on this elements' behaviour under cyclic load, as well as, to establish a relation between experimental data and the current European code prescriptions used to design these systems.

Seismic structural design has made considerable progresses in recent years. In spite of the evolution of understanding of structures' behaviour during earthquake events, the same has not happened for non-structural elements, consequently, code prescriptions may be limited when concerning the design of these elements. Nonetheless, currently, the study of the safety of these elements has taken an important role in structural engineering, not only to improve safety of buildings but also to minimize economical losses due to earthquake events. In fact, over the years, the economical weight of non-structural elements has become increasingly relevant when compared to the structural elements. Additionally, non--structural elements may be of particular importance in critical buildings, such as hospitals that should be fully functional after a seismic event.

As elucidated by their own definition, non-structural elements are components that only generate inertia forces and that are supported by structural elements. In this sense, the connection between these two types of elements, plays a critical role on their safety, in other words, seismic safety of non-structural elements is strongly related to the safety of their anchorage systems.

Several difficulties arise when seeking to safely design non-structural elements under seismic loading. First, earthquake loads are generally not acting directly on these elements. This means that, it is vital to understand how the load propagates from the structural elements to the non-structural ones. Because the load is transferred between different components, it is important to understand the amplifi-

cation of the response of non-structural components depending on the action subjected to the structural component. To this matter, dynamic analysis tools may be valuable to predict their response.

Nevertheless, in structural engineering a wide range of non-structural elements can be found. Besides the fact that these elements have remarkably different functions and characteristics, making it difficult to systematize their design, experimental testing may be expensive and time consuming. Consequently, the knowledge on the behaviour of these systems is a topic to be developed.

Apart from the estimation of the actions on these elements also the behaviour of the anchoring system needs to be studied. Recently, research on the behaviour of anchors under seismic loading has been made, however, most of these investigations are focused on metal anchors placed in concrete supports. Hence, behaviour on different base materials, like masonry, and made of different materials, such as plastic anchors, is still to be further developed. Furthermore, there are only standardized tests for metal anchor in concrete, consequently, it may be difficult to compare results on differently performed analysis.

The present dissertation starts by introducing current studies on this matter, as well as, some of the present code prescriptions used to design non-structural elements. At the end of the first chapter a more detailed look will be made on specific testing protocols used for the system studied in this analysis - façade cladding systems. Moreover, a simple introduction to dynamics of structures is made in order to present the analytical techniques used to perform this analysis.

After, the test layout used to acquire the experimental data is specified, focusing on the design of the system's components and on the protocols defined to study the system's behaviour. This study was composed by two groups of tests: the first regarding tests on a framed wall under dynamic loading and the second consisting on single fasteners' tests. Furthermore, the measurement devices' layout is detailed and the complete test program is presented.

Subsequently, the test results are presented allowing the estimation of dynamic parameters of the system, such as its natural frequency and damping ratio. Additionally, through single fastener testing, these elements' capacity and stiffness can be estimated. A comparison between predicted and experimental actions on anchors is performed.

Finally, with the previous results in mind a dynamic analysis through simplified models is performed and combined with results coming from a frequency domain analysis of the system's behaviour. Specifically, an inquiry is executed on the definition of seismic load acting on the cladding element, as well as, on the distribution of forces on the fasteners. Finally the results from this study are compared with prescriptions made by the European code.

Chapter 2

State of The Art

2.1 Introduction

According to Vijayanarayanan, Goswami, and Murty (2012) when dealing with a building two types of elements can be analysed: Structural Elements (SEs) which carry all earthquake induced inertia forces generated in the building to the foundations and Non-Structural Elements (NSEs) defined as items of buildings, supported by Structural Elements which only generate inertia forces, but do not carry them down to foundations. When speaking about seismic safety of structures it is meant not only of people but also safety of its contents for the predetermined seismic action. Depending on the non-structural element considered it may influence both the safety of people as well as contents.

In the past years a lot of improvement has been made in certain countries with advanced practices of earthquake safety, however although the loss of life has been minimized due to structural collapses, the economic set back due to lack of safety of NSEs is still large. Such damage have major social or economical impact, particularly in critical buildings like hospitals or commercial buildings. Even in urban buildings earthquake losses due to the failure of NSEs are on the rise, in fact, according to Miranda and Taghavi (2003) non-structural elements are a major part of the total investment in the United States, in figure (2.1) some typical buildings are analysed. According to Filiatrault and Sullivan (2014) damage to NSE occurs at seismic intensities much lower than the ones requires to produce structural damage.

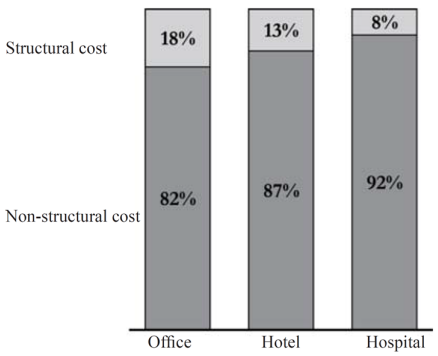

Figure 2.1: Relative investments in typical buildings (in Miranda and Taghavi (2003))

According to most authors, such as Salawdeh and Goggins (2016), Abdel-Mooty, Ahmed, and Mahmoud (2015), Filiatrault and Sullivan (2014), Mahrenholtz and Pregartner (2016), NSEs can be organized into three different groups depending on their geometry and functionality:

1. Architectural Components - built-in non-structural elements that form part of the building, such as cladding, ceilings, chimneys, among others;
2. Mechanical, Electrical and Plumbing - built-in non-structural elements that form part of the building, such as pumps, air handling units, distribution panels, among others;
3. Building Contents - non-structural components belonging to its occupants such as furniture, storage units, computers, among others.

In the present document special attention will be made to architectural components, more specifically to façade cladding.

2.2 Dynamics of Structures

Clough and Penzien (1975) describe the term dynamic as simply time-varying, thus, dynamic analysis of a structure can be viewed as an analysis where the actions on a structure vary in time in terms of magnitude, direction or position. Consequently also the structure's response, such as deformations and stresses, is dynamic. This means that, unlike a static problem, a dynamic problem does not have a single solution but a set of succession of solutions throughout the time domain of the analysis, which makes this analysis a more complex and time-consuming analysis than a purely static one.

Moreover, Clough and Penzien (1975) set these two types of analysis apart with the definition of equilibrium of the structure, while in a static analysis the structure's response is equilibrating the external actions, in a dynamic problem it must also equilibrate the inertia forces resulting from the accelerations imposed to the structure, in this sense, the inertial properties of the structure play a massive role on its analysis. If, for on hand, the motions are so slow that the inertia forces are negligible, the analysis made for any instant can be assumed purely static. However if this inertial forces are a significant part of the total load equilibrated by the structure, then a dynamic analysis must be performed.

The same authors define two different approaches when dealing with a dynamic problem: deterministic and non-deterministic, being the choice between the proper type of analysis basically dependent on how the dynamic action is defined. The first is used when the time-history of the action is completely defined and known, therefore the structural response can be obtained through a deterministic approach. However in most practical cases, such as earthquakes or wind loading, the time variation of the load is not completely defined, hence only statistic information can be used and the response of the structure to the random action will not be deterministic but statistically defined.

2.2.1 Discretization and Equations of Motion

As stated before, when dealing with a dynamic problem, inertial forces need to be considered, however this poses a problem since these forces are dependent on the motion of the structure, which in

time is also dependent on the inertial forces. This cause-effect cycle can only be solved through differential equations. Furthermore, because the mass of the structure is distributed continuously along its elements, both displacements and accelerations must be defined for each point in order to define completely the inertia forces.

If a solution for the different equations, and therefore a continuous solution for the inertia forces can be obtained for extremely simple structures, it would be practically impossible for regular structures and therefore it is normally adopted a discretization method of the structure in order to greatly simplify this analysis. Several types of discretization methods can be used, such as the Finite-Element method or the generalized displacements approach, however in the present document a more detailed description will be made of the lumped mass method.

The lumped mass method is more effective in structures where the large proportion of the mass is concentrated in some elements, this allows the distribution of the mass into some discrete points or lumps, thus, the inertia forces can be developed only at these points as well as both acceleration and displacements. The simplification of the problem can be grasped when considering the number of displacement components necessary to represent the effects of inertia forces - dynamic degrees of freedom. While in a continuous domain and infinite number of DOF should be defined, when dealing with a lumped mass system a finite number of DOF is attained. Figure 2.2 shows an example of distribution of inertial forces in a continuous and discretized system.

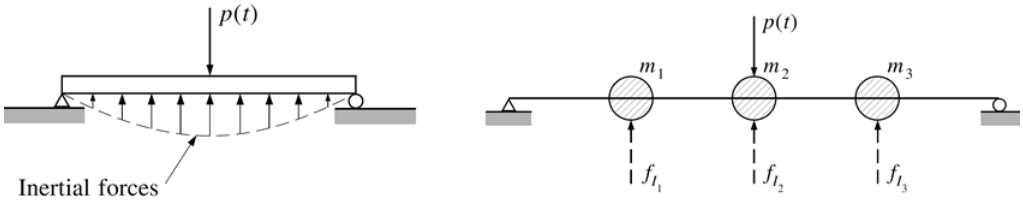

Figure 2.2: Continuous vs Lumped-Mass System (adapted from Clough and Penzien (1975))

The primary objective of a structural-dynamic analysis is the determination of the displacements time-history when the structure is subjected to a dynamic action. In order to define this response the formulation of a set of mathematical expressions defining its displacements can be set. These expressions are called equations of motion of the system and its definition is one of the most important parts of solving the dynamic problem. Several methods can be used to write these equations, however for the purpose of this work special attention will be given to the direct equilibrium definition through the d'Alembert's principle.

As explained by Chopra (1995), this principle is particularly appealing to structural engineers since is based on the notion of a fictitious inertia force which should be considered acting on the system. Therefore, the principles of static analysis can be used to develop the equation of motion through a free-body diagram of the moving mass stating that, with the fictitious inertia forces included, the system must be in equilibrium at any given time instant.

These forces can be simply computed with the support of Newton's second law of motion that states, as Clough and Penzien put it, that the rate of change of momentum of a mass m is equal to the force

acting on it $f(t)$ (equation 2.1), where $v(t)$ is the position vector of the mass. In other words, since mass is normally considered constant in time in structural engineering, that the force is equal to the product between mass and acceleration, v̈(t), as expressed in equation 2.2.

$$f(t) = \frac{d}{dt}\left(m\frac{dv}{dt}\right) \tag{2.1}$$

$$f(t) = m\frac{d^2v}{dt^2} \equiv m\ddot{v}(t) \tag{2.2}$$

The last expression 2.2 can also be written as show in 2.3 in which case the second term $m\ddot{v}(t)$ represents the inertia force resisting the acceleration of the mass. It is this concept of a resisting force proportional to the acceleration that is known as the d'Alembert's principle.

$$f(t) - m\ddot{v}(t) = 0 \tag{2.3}$$

In this expression 2.3 $f(t)$ can be considered as several types of forces, defined by Clough and Penzien (1975) as elastic constraints resisting displacements, viscous forces related to velocities or independent external loads, acting on the mass point where equilibrium is expressed.

2.2.2 Single Degree of Freedom Systems

The simplest model of a dynamic system is a single degree of freedom system (SDOF), in which only one component of dynamic displacement is independent. The simplest model of a SDOF system can be described, as in Clough and Penzien (1975), as one where all the essential physical properties are concentrated in a single element. These parameters include its mass, elastic properties, damping mechanisms and external source of excitation. A scheme of an idealized SDOF system can be seen in figure 2.3

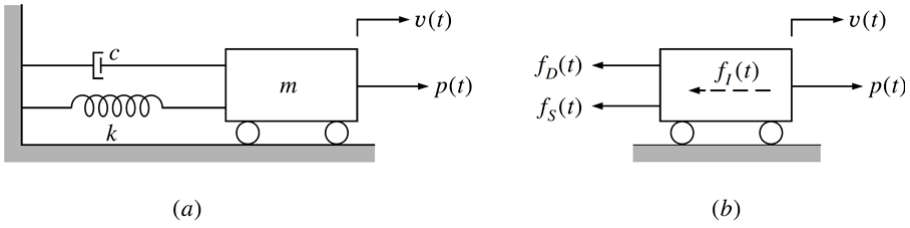

Figure 2.3: Idealized SDOF system: (a) basic components; (b) forces in equilibrium (in Clough and Penzien (1975))

As seen above, the rigid block includes the entire mass of the system m under the action of an time-varying external load $p(t)$. Rollers constrain the block, therefore only a horizontal displacement is allowed, $v(t)$, which constitutes the only degree of freedom of the system. The elastic resistance to displacement is represented by the linear spring with stiffness k, while c represents the damping of the system.

It is important to introduce the definition of the physical quantity represented by c. Chopra (1995) defines damping as the process that leads to a decreasing amplitude of vibration. Several mechanisms

can lead to this behaviour by dissipating both kinetic and strain energy and in fact, when testing the free vibrations of a real structure (vibrations with no external loading) it can be observed this decay in motion. This physical property of the system can be described through several models being the most common one, due to being the less mathematically cumbersome, the viscous damper, where the damping force is proportional to the velocity, $\dot{v}$, with a proportionality constant c - damping constant - as expressed in equation 2.4. This physical phenomena will be explored more in detail further on.

$$f_D = c\dot{v} \tag{2.4}$$

With the support of d'Alembert's principle and considering the actions shown in figure 2.3 it is possible to compute the equilibrium on the rigid block (equation 2.5)

$$f_I + f_D + f_S = p(t) \tag{2.5}$$

Where $p(t)$ represents the applied dynamic load, f_I the inertial force, f_D the damping force and f_S the elastic force. The latest is obviously proportional to the displacement of the rigid block, being the proportionality constant equal to k. Considering the definition for the forces involved in this equilibrium, equation 2.5 can be transformed into the differential equation 2.6:

$$m\ddot{v} + c\dot{v} + kv = p(t) \tag{2.6}$$

Expression 2.6 represents the equation of motion of an idealized single degree of freedom system.

2.2.3 Free Vibrations of a SDOF system

Normally when solving a dynamic problem the solution of the second order differential equation presented in the previous section is obtained through the combination of a general solution and a particular solution. The general solution describes the behaviour of the system under no external actions it while the particular solution is related to the actions on the system.

When dealing with an homogeneous equation of motion the term free vibrations is used, in other words, it expresses the behaviour of the system independently from the actions that may act on it. In this sense the solution for expression 2.7 is seek.

$$m\ddot{v} + c\dot{v} + kv = 0 \tag{2.7}$$

The study of free vibrations of a dynamic system enables an understanding of its dynamic behaviour. Special emphasis is made on the fact that this analysis will allow an estimation of the eigen frequency of this system. As it will be exposed later on, the relation between the natural frequency of the system and the load frequency will greatly influence the response of the system. Although for damped systems the method to compute this parameter can be complex, when dealing with an undamped system it is relatively simple to attain it. An so, in practical works it is frequent to neglect the damping of the structure.

According to Chopra (1995) damping has an effect of lowering the natural frequency from ω_n to ω_D and lengthening the natural period from T_n to T_D, however these effects are negligible for low damping ratios (under 20 %), a range in which most structures belong as seen in picture 2.4:

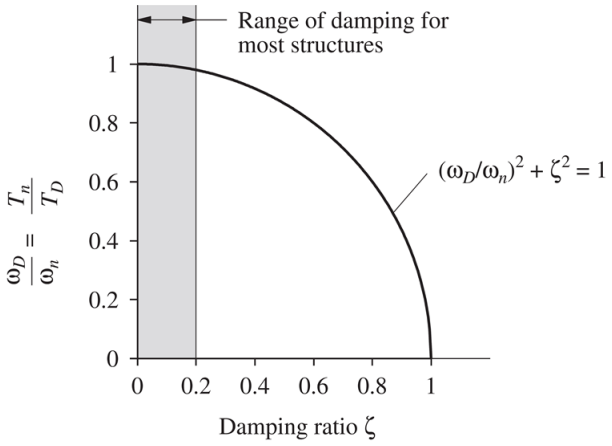

Figure 2.4: Effects of damping on the natural vibration frequency (in Chopra (1995))

Consequently the natural frequency of a single degree of freedom system can be estimated as expressed in equation 2.9 where ω_1 is the natural circular frequency (in rad/s) and f_1 is the natural frequency (in Hz)

$$\omega_1 = \sqrt{\frac{k}{m}} \tag{2.8}$$

$$f_1 = \frac{1}{2\pi}\omega_1 \tag{2.9}$$

It can be seen that these parameters depend on the mass m of the system and the stiffness k, defined when studying the equation of motion of the structure.

2.2.4 Earthquake Dynamic Loading

When defining the equation of motion of a system the parameter f(t) was set as generic action on the structure. So it is important to understand how this action can be defined. In the present work it is of particular importance the behaviour of the system not to a dynamic force but to the motion of its support points. This analysis is analogous to the analysis made for an earthquake dynamic loading.

Chopra (1995) uses three quantities to derive the equation of motion for these type of loading: $v_g(t)$ the ground displacement to which the structure is subjected, v(t) the relative displacement between the structure and the ground and $v_t(t)$ the total displacement of the structure. The following relation (equation 2.10) is valid.

$$v_t(t) = v_g(t) + v(t) \tag{2.10}$$

It is shown in equation 2.5 the relation between the loads acting on the structure. For the case where the external forces are zero, the dynamic equilibrium can be written as 2.11

$$f_I + f_D + f_S = 0 \tag{2.11}$$

Both the elastic and damping force are related with the relative displacement between the ground and the structure, however the inertia force is related with the total displacement of the structure and so f_I can be written as 2.12

$$f_I = m\ddot{v}_t(t) = m\left[\ddot{v}_g(t) + \ddot{v}(t)\right] \tag{2.12}$$

Considering the previous definition of inertia force the equation of motion can be rewritten as shown in 2.13

$$m\ddot{v} + c\dot{v} + kv = -m\ddot{v}_g \tag{2.13}$$

Chopra (1995) defines the quantity $-m\ddot{v}_g$ as the effective earthquake force, proportional to the ground motion acceleration and to the mass of the structure. Note that this reasoning is valid for any support excitation, independently on the cause for the ground motion.

As Clough and Penzien (1975) point out, the minus sign means that the force is opposed to the ground acceleration, however, in practise, the analysis is interested on the computation of the maximum absolute value of displacement v(t) and in these cases the minus sign can be removed from the effective loading term.

2.2.5 Frequency Domain Analysis

Several methods can be used in order to compute the dynamic response of a system. These analysis can be generally divided into two main types: time domain analysis, which includes methods such as the step-by-step procedure or the numerical analysis of Duhamel's integral, and the frequency domain analysis.

For the purpose of this study an analysis on the frequency domain will be used and so small remarks on this type of analysis will be made. The frequency domain analysis is specially useful for particular systems, for example when the stiffness of the system is dependent on the frequency of the action or for the dynamic analysis of structures interacting with unbounded media (in Chopra (1995)).

As explained by Clough and Penzien (1975), the formal application of the frequency domain analysis procedure is limited to the cases for which the Fourier transform of the applied load functions are available. However, the formal computation of these integrals in a practical case is generally a tedious process, in this sense, it is common to use the discrete Fourier transform which allows numerical methods with a higher efficiency. Moreover the Fourier transform will be computed for time steps, which length should ensure the stability and accuracy of the method, allowing computational programs to be used.

In this sense, data gathered in the time domain can be used to assess the structure's behaviour depending on the frequency characteristics of the excitation, with no loss of information. The relation between time and frequency can be computed with the definition of discrete Fourier transform:

$$G\left(n\Delta f\right) = \sum_{k=0}^{N-1} \hat{g}\left(k\Delta t\right) e^{-i2\pi nk/N} \tag{2.14}$$

where $G(n\Delta f)$ is the function to be computed on the frequency domain and $\hat{g}\left(k\Delta t\right)$ is the discrete time

domain information to be transformed to the frequency domain.

2.2.6 Transfer Function

Clough and Penzien (1975) define functions that represent the input-output relation as transfer functions. These functions characterize the stationary output process in terms of its corresponding input process.

Being the scope of this work's analysis to infer the characteristics of a time-dependent physical problem considering the fact that it is not deterministic but probabilistic, the analysis should consider a stochastic process, in other words, an aleatory phenomenon that depends on deterministic parameters, such as time and spacial coordinates.

Moreover, as Clough and Penzien (1975) explain, uncontrollable random variables are always present when dealing with real systems, consequently also the computed transfer function will have random characteristics. However, in vibration analysis, this random property is small when compared to the randomness of the input, and therefore can be neglected. In this way it can be assumed as a deterministic function.

As stated before, both the input and output can be considered as stochastic processes, hence a stochastic analysis should be used when dealing with them. As Clough and Penzien (1975) demonstrate, when the transfer function and either the power spectral density or the autocorrelation function of the input are known, then the output can be fully characterized. On an analogous reasoning, if both the input and the output are known, then the transfer function can be computed. This relation is particularly useful if experimental testing is done.

To that end, assuming a know set of data from both the input and output, the power spectral density function can be computed according to expression 2.15.

$$S_x(f) = \lim_{T\to\infty} \frac{1}{2T} E[|\tilde{x}^{(j)}(f,T)|^2] \tag{2.15}$$

where $\tilde{x}^{(j)}$ is the parameter to be studied.

Accordingly, the transfer function $H(f)$ can be computed based on the previous concept simply as expression 2.16 shows:

$$H(f) = \sqrt{\frac{S_{xfacade}(f)}{S_{xwall}(f)}} \tag{2.16}$$

2.2.7 Frequency Response Curves

A plot of the amplitude of a response quantity as a function of the excitation frequency is called a frequency response curve. Hence, the previous developed transfer function, where the input and output are, respectively, the acceleration of the action and the acceleration of the system's response, can be seen as an acceleration's frequency response function. This function will allow the estimation of the amplification of the output, depending on the characteristics of the input, more specifically, on the relation between the frequency of the action on the structure and the natural frequency of the system.

If the damping of the system has a negligible influence on the natural frequency of the system, the same is not correct in terms of the magnification factor. Plots which explicitly relate the amplification factor with the excitation are dependent on the damping of the structure, as observed in figure 2.5.

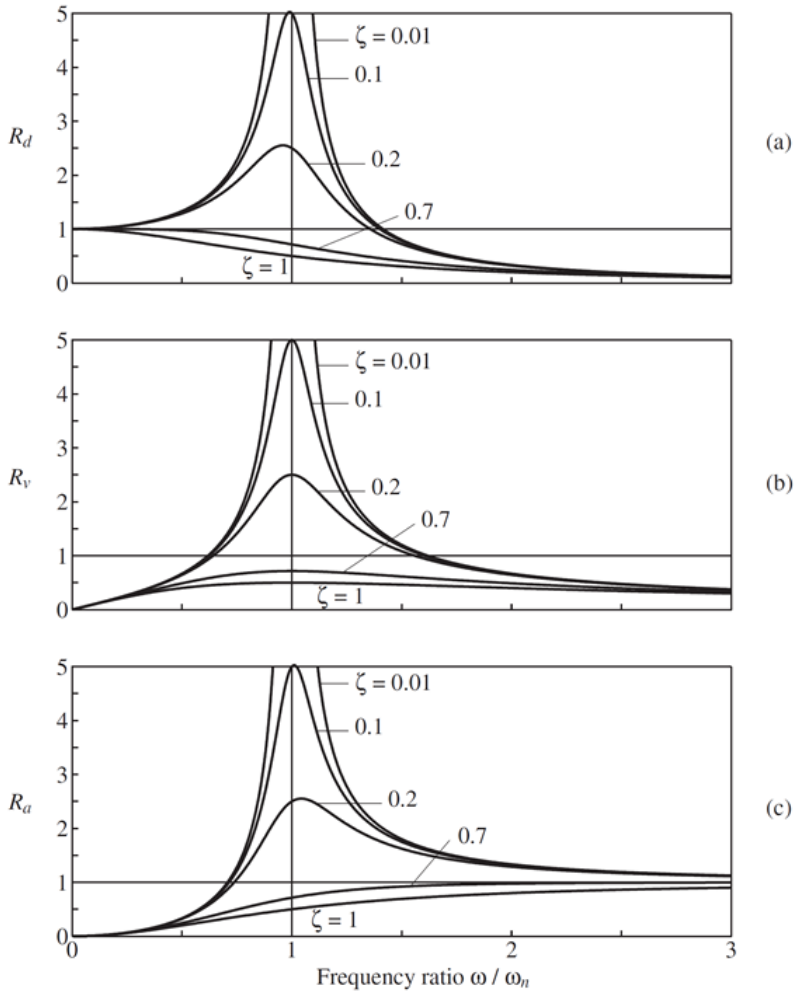

Figure 2.5: Deformation (a), velocity (b), and acceleration (c) response factors for a damped system excited by harmonic force (in Chopra (1995))

Frequency response curves have three main regions on the excitation frequency scale. One under the resonant state, the resonant state and one above it. It can be seen that on a resonant state, where the frequency ratio is close to one (for damping factors inside the scope of this study), the response is extremely sensitive to the damping factor and, for small damping coefficients, the static response can be increased of factors several times larger than one. Consequently the dynamic response can be much higher than the static one. Hence, to understand this amplification of the response a correct estimation of the damping of the structure should be made.

Experimental Definition of Damping Ratio

Several methods are known to estimate the damping ratio of a structure. In this section the logarithmic decrement is considered. This method relies on experimental data from forced vibration tests.

A relation between two successive peaks of damped free vibration and the damping ratio can be

found through the logarithmic decrement, δ. The ratio of the displacement at time t to its value a full vibration period later is independent of t. The natural logarithm of this ratio is called the logarithmic decrement and is related to the damping ratio, for small values of ζ as stated in equation 2.17. The range on which this approximate solution is valid can be seen in figure 2.6.

$$\delta = \ln\left[\frac{v(t)}{v(t+nT_D)}\right] = \frac{2\pi\zeta}{\sqrt{1-\zeta^2}} \approx 2n\pi\zeta \tag{2.17}$$

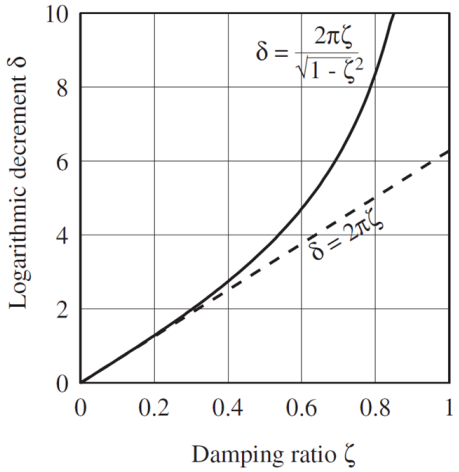

Figure 2.6: Exact and approximate relations between logarithmic decrement and damping ratio (in Chopra (1995))

Acceleration Response Factor

Once the damping ratio of the structure is known it is possible to estimate the amplification factor. For small damping systems, the maximum amplification of the acceleration, A_a occurs when the excitation frequency is approximately equal to to the eigen frequency of the system and, according to Chopra (1995), it can be related to the damping ratio with expression 2.18, approximated for small values of ζ.

$$A_a = \frac{1}{2\zeta\sqrt{1-\zeta^2}} \approx \frac{1}{2\zeta} \tag{2.18}$$

2.3 Effects of Earthquake on NSEs

Earthquake resistant design philosophy currently agreed on requires that the consequences of the earthquake shaking on the elements should depend upon the level of earthquake as well as building type. Obviously, higher level earthquakes lead to lower performance standards and critical buildings have less damage tolerance than normal buildings. This philosophy can also be applied to NSEs as shown in the table 2.1.

Table 2.1: Expectation of SEs and NSEs During Different Levels of Earthquake Shaking (in Vijayanarayanan, Goswami, and Murty (2012))

Building Type	Level of Earthquake Shaking					
	Structural Elements			Non-Structural Elements		
	Minor (or frequent)	Moderate	Severe (or infrequent)	Low (or frequent)	Moderate	Severe (or infrequent)
Normal	No damage	No damage	No collapse	No damage	Some damage	-
Critical and Lifeline	No damage	No damage	Minor damage	No damage	Functional	No permanent damage

Being the previous expected levels defined as:

- No damage - The element should endure the load without damaging both of the element as well as of the elements attached to it.
- No permanent damage - The element may suffer some damage during the seismic event but it should remain on its elastic behaviour range.
- Minor Damage - The element may suffer minor damage that should not affect its safety or functionality.
- Some damage - The element may suffer damage that may affect its functionality but never its safety.
- Functional - The element and the elements attached to it may suffer permanent damage if it does not affect its functionality.
- No collapse - The element may suffer permanent damages that affect its functionality but it must not collapse.

Assuming this reasoning it is essential to see if the level of damage on the NSEs for different earthquakes respects the design expectations. Hence it is crucial to understand the effects that this action has on the elements. According to Vijayanarayanan, Goswami, and Murty (2012) there are two basic effects of earthquake shaking on NSEs:

1. That which causes sliding, rocking and toppling. Characteristic of stiff and heavy NSEs.
2. That which causes stretching compressing, shearing and swing by large amounts in translation and rotation. Observed in flexible and light NSEs if anchored stiffly to their supports.

Based on this effects it is possible to classify NSEs into two groups depending on how earthquake affects them and consequently on the design approach that is more suitable.

- Acceleration Sensitive NSE - sensitive to 1. Their connections should be designed for lateral inertia forces.
- Deformation Sensitive NSE - sensitive to 2. Are vulnerable to inter-storey drift and the connection should be designed for relative deformation actions between the ends of NSEs. Ideally no damage situation can be ensured in deformation-sensitive NSEs by designing them to accommodate the expected lateral deformation between their ends; the challenge is to estimate this relative deformation.

It is important to notice that some NSEs fall under both categories with one of the effects being more dominant (primary effect), while the other is considered a secondary effect. In this situations the design of these elements and their connection to the structure should consider both effects. Failure of the non-structural elements can also be defined according to its consequences: the direct lost of a NSE is called primary hazard if the NSE can cause direct threat to life or impairs the function of the NSE; and secondary hazard if it can cause loss to other NSEs or failure of the function of the building.

2.3.1 Performance of NSE

When designing a non-structural element two main aspects should be considered. First the effects of the earthquake directly on the element that may damage it; second its connection with the adjoining structural element that must resist the actions induced by the shaking. The definition of the later actions is crucial not only to ensure the safety of the NSEs but should also be considered when designing the structural element since it will cause additional forces.

Generally structures are designed to undergo acceptable damage, depending on its function and the earthquake level, so when discussing the design of structural elements it is common to talk about performance-based design which recognizes four qualitative levels of performance for building's structure. Similarly we can define a performance-based design for NSEs. For them, Vijayanarayanan, Goswami, and Murty (2012) conceives four performance levels, namely:

1. Fully Functional performance level (FF) - The element is shaken by the earthquake but its function is not, even marginally, impaired, it suffers no damage.

2. Immediate Use performance level (IU) - The NSE is shaken within its linear range of behaviour and suffers no damage, even tough minor damages can occur to elements attached to it.

3. Dysfunctional State performance level (DS) - The NSE is shaken severely in its linear range and even though it is not damaged, it cannot be used due to failure of units attached to it;

4. Damage or Collapse performance level (DC) - The element is shaken severely in its non linear range of behaviour and it is impaired.

Once again the performance for which the structure should be designed will depend on the building type and, for the same action, higher performance levels should be prescribed to critical and lifeline buildings and contents as seen in figure (2.7) where the roof deformation, Δ, is related with the base shear, H, for four different intensities of earthquake shaking.

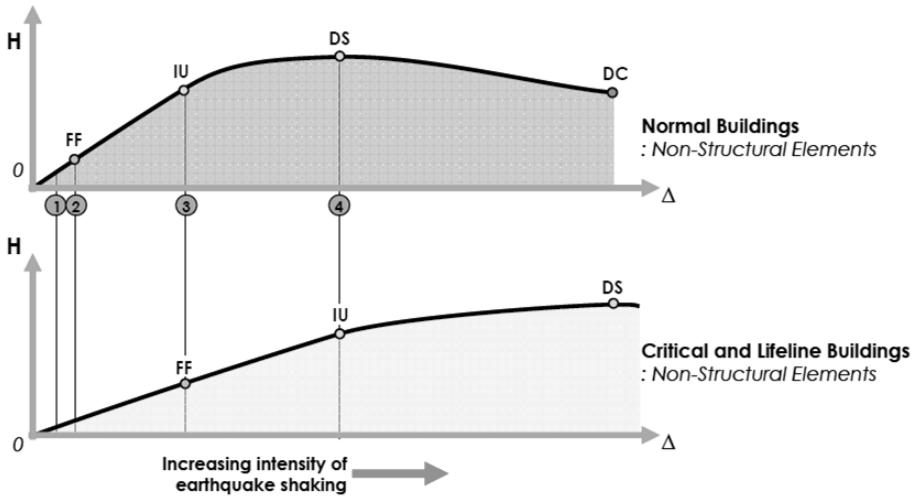

Figure 2.7: Performance Levels for Non-structural Elements (in Vijayanarayanan, Goswami, and Murty (2012))

2.4 Fasteners in Structural Engineering

2.4.1 Types of Fasteners

According to Hoehler (2006) fasteners can be subdivided according to the way they are installed and their load transfer mechanism. For the first parameter it can be distinguished between cast-in and post--installed systems depending on whether they are installed prior to material casting or into a hardened anchorage material, respectively.

Regarding the load transfer mechanism Eligehausen, Mallée, and Silva (2006) identify three different processes: mechanical interlock, friction or bond. Commercial anchors may transfer the load through one mechanism or through a combination of them. The principles of these mechanisms can be summarized as follows, being figure 2.8 a schematic view of the tension load transfer.

- Mechanical Interlock - The transfer of load happens by bearing the fastener on the base material;
- Friction - the fasteners geometry allows an expansion force to be created which in turn generates friction forces between the fastener and the sides of the drilled hole;
- Bond - the load is transferred by means of a chemical interlock, in other words, through some combination of adhesion and micro-keying.

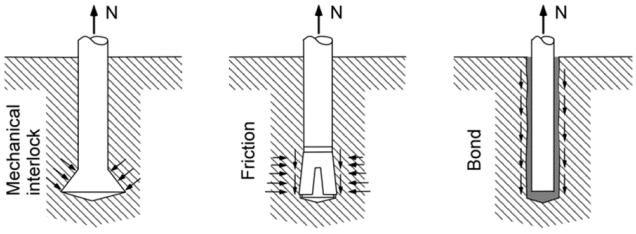

Figure 2.8: Tension load transfer mechanisms (in Hoehler (2006))

2.4.2 Post-installed Fasteners

Special attention will be made to post-installed fasteners. The main advantage of these anchors is the flexibility for planning and executing a connection. The fact that their installation is made on hardened material makes these fasteners an interesting choice when retrofitting existing structures, for example in seismic strengthening and rehabilitation.

Hoehler (2006) describes two procedures to install these fasteners, either by direct installation, with powder cartridges or pneumatic action, or through insertion into a pre-drilled hole. However, according to this author the majority of post-installed fasteners requires drilling and therefore, the increasing use of post-installed fasteners can largely be attributed to advances in the drilling technology. Moreover, when discussing the installation of these fasteners the author differentiates three installation configurations, schematically shown in figure 2.9.

- Pre-positioned - installed in the anchorage material before the element to be fastened to is attached;
- In-place - installed through the element to be fastened. The fixture can be used as a drilling template;
- Stand-off - the item to be fastened is mounted at a distance from the surface of the base material.

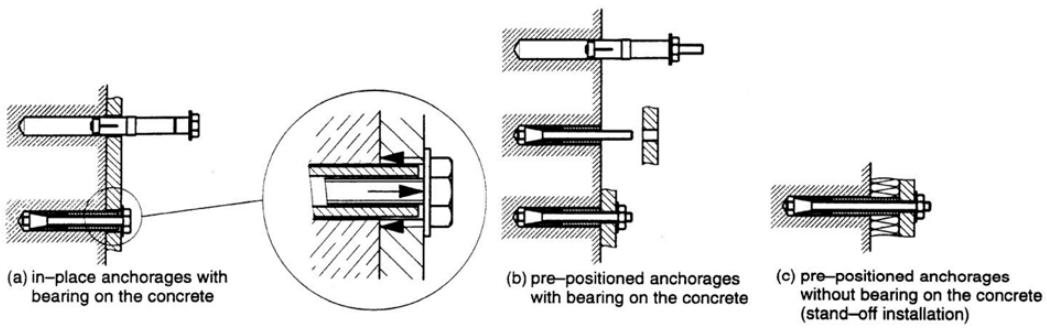

Figure 2.9: Installation configurations (adapted from EOTA (2013c))

2.4.3 Plastic Anchors for Multiple Use in Concrete and Masonry

The design of post-installed fasteners is firmly connected with the base material where the anchor is installed. European guidelines are available to provide the design methods for a range of fasteners in a spectrum of base materials. For the intent of this document concrete and masonry will be analysed and focus will be made plastic anchors.

According to ETAG 020 EOTA (2012) plastic anchors consist of an expansion element and a polymeric sleeve which passes through the fixture. These two elements should behave as a unite and should have approximately the same length. These fasteners work as expansion anchors where the polymeric sleeve is expanded by hammering or screwing of the expansion element, pressing the sleeve against the wall of the drilled hole.

It is the mechanism through which the sleeve is expanded that separates the two types of plastic anchors covered in ETAG 020 EOTA (2012):

- Screwed-in Anchors (figure 2.10)
- Hammered-in Anchors (figure 2.11)

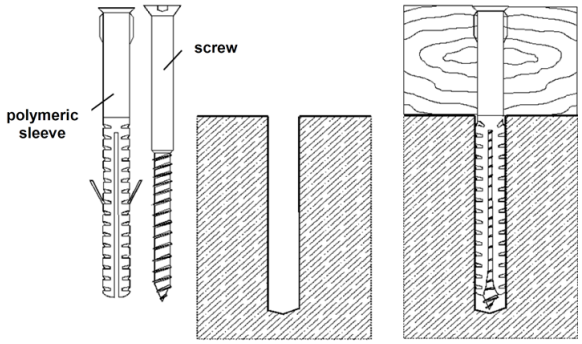

Figure 2.10: Screwed-in Plastic Anchor (in EOTA (2012))

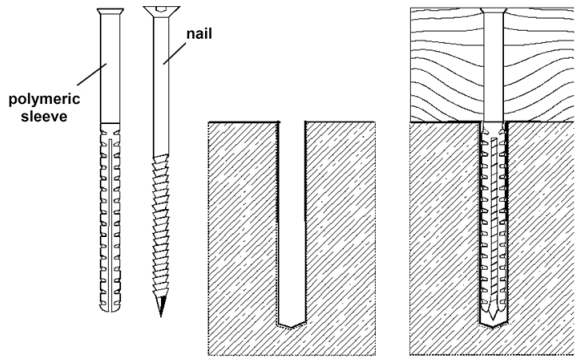

Figure 2.11: Hammered-in Plastic Anchor (in EOTA (2012))

For the design of anchors it is crucial to understand the failure modes linked to each base material. Hence, the European guidelines provide the description of failure modes for each case as well as verifications that should be made to prevent failure of the anchor. Regarding the European guideline for plastic anchors, EOTA (2012), it is important to remark that it only develops design methods for plastic anchors subjected to static or quasi-static loads and it is not applicable to plastic anchors loaded in compression or subjected to fatigue, impact or seismic actions.

The design methods for plastic anchors in concrete and masonry are exposed in annex C of ETAG 020 EOTA (2010) for static or quasi-static loading. When dealing with the failure of anchors it is important to be aware that their failure mechanism is dependent on the actions on the anchor and can be reached through both failure of the fastener or of the base material or a combination of both.

Anchors in Concrete

ETAG 020 EOTA (2010) prescribes, in annex C, the design for ultimate limit state for plastic anchors in concrete. The failure mechanisms depend on the load acting on the anchor and can be separated into failure due to tension loading and due to shear loading.

For the cases where tension load is analysed three types of failure are admitted: failure of the expansion element, pull-out failure and concrete cone failure. On the other hand, if shear load is studied the failure may occur through failure of the expansion element for shear loading with or without lever arm and concrete edge failure.

The resistance of the anchor should be verified both for purely tension and shear loading as well as for the combination of both.

Anchors in Masonry

Table 2.2: Characteristic resistance in masonry (use categories b, c and d) depending on visibility and condition of the joints (in EOTA (2010))

	1	2	3
1	**Joints**	**Characteristic resistance depending on the joints (a)**	
		joints are visible	**joints are <u>not</u> visible**
2	**filled with mortar (b)** (perpend/vertical and bed/horizontal joints)	F_{Rk}	$0{,}5 \cdot F_{Rk}$
3	**<u>not</u> filled with mortar (b)** (perpend/vertical joints)	$0{,}5 \cdot F_{Rk}$ **(c)** and $N_{Sd} \leq 2{,}0$ kN **(d)**	$0{,}5 \cdot F_{Rk}$ and $N_{Sd} \leq 2{,}0$ kN **(d)**
4	**interlocking units** (perpend/vertical joints)	F_{Rk}	$0{,}5 \cdot F_{Rk}$
5	**glued together** (only bed/horizontal joints in AAC)	F_{Rk}	$0{,}5 \cdot F_{Rk}$

(a) F_{Rk} = characteristic resistance given in the ETA for the individual masonry units

(b) The condition of the joint shall be determined from the design of the wall (e.g. joints of the wall are designed to be filled with mortar) or from a representative assessment for existing constructions.

(c) The characteristic resistance does not have to be reduced to $0{,}5 \cdot F_{Rk}$ if the minimum edge distance c_{min} to the vertical joints is observed. The minimum edge distance c_{min} is given in the ETA for the individual masonry units.

(d) N_{Sd} has to be limited to 2,0 kN to ensure that a pull-out of one brick of the wall will be prevented.

For anchors in masonry ETAG 020 EOTA (2010) does not explicitly defines the failure modes of the system. According to this document, the anchor's European technical assessment (ETA) should specify only one characteristic value of resistance F_{rk} which is independent of the load direction and failure mode. However some coefficients should be taken into account when computing the resistance of the fastener in a masonry wall. These coefficients are dependent on the joints of this element and are represented in table 2.2.

One special load case is distinguished, shear load with lever arm, in which case, the expressions used for failure in concrete should be used and resistance of the fastener will be the lowest between the characteristic resistance F_{rk} and the shear resistance V_{rk}.

2.5 Connections Between Non-structural and Structural Elements under Seismic Load

The safety of acceleration-sensitive non-structural elements is attained by designing them for the forces transferred due to the inertia of the element. In this sense, safety depends on the proper anchoring into the structural element. Hence, it is essential to design the connection for the expected lateral force or admissible displacement during the earthquake event. Seismic codes provide a lower bound estimate of the design lateral force for which the connections between the NSE and the adjoining SE should be designed for. This force is dependent on the acceleration at the point of attachment and the weight imparted to the connection. In Vijayanarayanan, Goswami, and Murty (2012) it is stated that the minimum force prescribed by the codes for the connection represents a higher percentage of weight in non-structural elements when compared with structural elements. Hence, a higher percentage of inertia is mobilized in NSEs which implies that even under minor shaking the forces on the NSEs can be significant.

As for the acceleration at the point of attachment of the NSE to the SE, it will depend on peak ground acceleration, dynamic response of the building and location of the element. The effect of dynamic amplification of the NSE relative to the fundamental natural period of the building should be considered, normally this is taken into account by a amplification factor. In theory, experimental tests using shaking tables are required to evaluate the the natural frequency of the NSE, however this is not feasible for all elements and so, codes tend to prescribe values for the parameters required for the computation of the forces in the connection.

Calvi (2014) states that in the case of a single degree of freedom supporting structure the peak acceleration of a system can be accurately computed as the ratio between the maximum seismic force imposed on the system and the system's mass. Due to dynamic amplification, the peak of an acceleration response spectrum occurs in correspondence with the natural frequency of the structure. Its value is typically equal to the peak ground acceleration multiplied by a dynamic amplification factor (DAF). Sullivan *et al.*, 2013 (in Calvi (2014)) proposes for this parameter expression (2.19):

$$DAF = \frac{1}{\sqrt{\left(1 - \frac{1}{\beta}\right)^2 + \zeta}} \tag{2.19}$$

where

$\beta =$ Ratio between the natural period of the element and the natural period of the supporting structure

$\zeta =$ Damping ratio

As Vijayanarayanan, Goswami, and Murty (2012) explains, the imposed inertia force and relative displacement on the connection depend on the intensity of the earthquake shaking and consequently the correct definition of this action is imperative for a safe and efficient design of these elements. Moreover, the optimal connection for a given system should consider not only the expected performance during and after an earthquake event, but also a minimum cost. If a connection that is stiffer than the optimal

solution increases its cost and may lead to damage of the NSE, too much flexibility will cause damage to both the NSE and the building, becoming a treat to safety.

2.5.1 Behaviour of Post-installed Anchors under Cyclic Loads

In Fröhlich et al. (2017) cyclic tests on post installed anchors in concrete were performed. According to the dynamic response of the structural elements, cracks in concrete open and close cyclically and so the tests on the post-installed anchors where performed under cyclic load and crack opening in order to analyse this effect on the anchor behaviour. It was clear that the load-displacement behaviour of the anchors was strongly affected by crack cycling. In this way, when performing the seismic design of these elements this dynamic behaviour should be considered and it is crucial for the manufacturers to investigate not only the static but also the dynamic proprieties of the anchors.

Salawdeh and Goggins (2016) characterize the seismic behaviour of connections through six proprieties:

1. Strength - the maximum force that can be resisted by the connection;
2. Ductility - ratio between maximum plastic deformation and the yielding deformation;
3. Dissipation - relation between the energy dissipated through the load cycles and the one in a perfect elasto-plastic cycle;
4. Deformation - ultimate deformation reached at failure;
5. Decay - loss of strength through the load cycles;
6. Damage - residual deformation after unloading.

These parameters can be estimated through monotonic and cycling tests. In this sense, several testing procedures are prescribed to study the seismic behaviour of post-installed metal anchors in concrete.

2.5.2 Code Provisions for Non-Structural Elements

There are several references that provide engineers with equations and simple rules to compute forces induced by earthquakes on non-structural elements. In Abdel-Mooty, Ahmed, and Mahmoud (2015) different seismic international codes and specifications are analysed. These codes are based on seismic intensity; fundamental period for the SEs and NSEs; soil condition; height of the NSEs above the base of the building as well as total height of the building. It has been shown that the dynamic characteristics of the building have a considerable effect on the response of non-structural elements. Hence, it is important to identify the dynamic proprieties of both the supporting structure and of the NSE before investigating the response of the NSE. In Abdel-Mooty, Ahmed, and Mahmoud (2015) the seismic safety of non-structural elements is evaluated considering different code provisions. As an example Eurocode 8 CEN (2014) and the international Building Code IBC (2012) are presented, both

prescribe the Equivalent Lateral Force Method where the seismic force is computed as a percentage of the weight of the NSE.

Eurocode 8

Soil Factor, non-structural element's self-weight, flexibility and importance factor are considered in this code. Also the code requires realistic modelling for very important and dangerous non-structural elements by using floor response spectra. For other elements Eurocode recommends design seismic loads, F_a as (2.20) in CEN (2014):

$$F_a = \frac{S_a \gamma_a}{q_a} W_a \tag{2.20}$$

with

$$S_a = \alpha \times S \left[\frac{3\left(1 + \frac{Z_a}{H}\right)}{1 + \left(1 - \frac{T_a}{T_1}\right)^2} - 0.5 \right] \geqslant \alpha \tag{2.21}$$

where,

$F_a =$ Horizontal seismic force, acting at the centre of mass of the non-structural element in the most unfavourable direction;

$q_a =$ Behaviour factor for non-structural elements;

$W_a =$ Weight of the non-structural element;

$\gamma_a =$ Importance factor;

$\alpha =$ Ratio between design ground acceleration a_g and the ground acceleration g;

$S =$ Soil factor;

$Z_a =$ height of the non-structural element above the base of the building;

$H =$ Total height of the building;

$T_a =$ Fundamental period of the non-structural element;

$T_1 =$ Fundamental period of the building.

It is important to better understand the meaning of parameter q_a. According to CEN (2014) the behaviour factor is used to reduce the forces obtained from a linear analysis. In this way, the non-linearity of the structural response is taken into account indirectly allowing the design methods used for linear analysis. Moreover, the energy-dissipation of the system is related to this non-linear behaviour and, consequently, the efficiency of the structure's design is dependent on the choice of behaviour factor.

When using equation 2.21 it can often be difficult to estimate the fundamental vibration period of the non-structural element, with this in mind in EOTA (2013a) a pragmatic approach to the computation of the equivalent force is suggested where the parameter A_a - seismic amplification factor - computed as seen in equation 2.22 is prescribed for several elements, as shown in table 2.3

$$A_a = \frac{3}{1 + \left(1 - \frac{T_a}{T_1}\right)^2} \tag{2.22}$$

Table 2.3: Values of q_a and A_a for non-structural elements (in EOTA (2013a))

Type of non-structural element	q_a	A_a
Cantilevering parapets or ornamentations	1,0	3,0
Signs and billboards		3,0
Chimneys, masts and tanks on legs acting as unbraced cantilevers along more than one half of their total height		3,0
Hazardous material storage, hazardous fluid piping		3,0
Exterior and interior walls	2,0	1,5
Partitions and facades		1,5
Chimneys, masts and tanks on legs acting as unbraced cantilevers along less than one half of their total height, or braced or guyed to the structure at or above their centre of mass		1,5
Elevators		1,5
Computer access floors, electrical and communication equipment		3,0
Conveyors		3,0
Anchorage elements for permanent cabinets and book stacks supported by the floor		1,5
Anchorage elements for false (suspended) ceilings and light fixtures		1,5
High pressure piping, fire suppression piping		3,0
Fluid piping for non-hazardous materials		3,0
Computer, communication and storage racks		3,0

International Building Code

International Building Code 2012 calculates the non-structural elements' force, F_p, as (2.23), in IBC (2012):

$$F_p = \frac{0.4 a_p S_{DS} I_p}{R_p} \left(1 + 2 \times \frac{z}{h_t}\right) W_p \tag{2.23}$$

and

$$0.3 S_{DS} I_p W_p \leq F_p \leq 1.6 S_{DS} I_p W_p \tag{2.24}$$

where

$a_p =$ Component amplification factor to account for flexibility of the NSE;

$W_p =$ Weight of the non-structural element;

$S_{DS} =$ Spectral acceleration at short period structures $= 2/3 S_{MS}$. $0.4 S_{DS}$ represents the peak ground acceleration;

$S_{MS} =$ Mapped considered earthquake spectral response acceleration for short periods;

$R_p =$ Response modification factor;

$I_p =$ Importance Factor;

$z =$ Height of the point of attachment of component with respect to the base;

$h_t =$ Average roof height of the building with respect to the base.

Limitations to the Provisions

Hoffmeister, Gündel, and Feldmann (2011) states that there are several deficiencies with the current provisions prescribed by both the Eurocode 8 and International Building Code regarding the design of non-structural elements. First, on the design of the seismic forces acting on the component it is assumed the first fundamental period and linear shape of the forces, which is not true for irregular structures where torsional effects can have a significant influence. Additionally only the peak ground acceleration and soil factor are considered, instead of the real response of the supporting structure with regard to the design response spectrum. According to Calvi (2014), the limitations of existing methodologies stems from the inappropriate way of accounting for the behaviour of the supporting structure, namely its higher modes and its non-linear response. Moreover, none of the codes seem to account for the elastic damping of the component to be designed, which was in fact shown to have a major influence on the demand, in Sullivan, Calvi, and Nascimbene (2013).

Moreover there is currently no guidance on how to consider the interaction between the supporting structure and the non-structural component so, in some practical design situations, decoupled analyses are performed based on a cascading approach, being the most common the floor response spectrum. For important non-structural elements a more accurate analysis should be made and a floor response spectrum (FRS) can be used. The design acceleration spectrum at the base of the building is used to define the acceleration spectrum at the base of the NSE (FRS) and to determine the acceleration response spectrum at the level of the connection. This method was developed in the 1960's for the study of secondary systems in power plants and since then, attempts have been made to design simplified yet reliable methods to construct these spectra.

2.5.3 Test Protocols for Fasteners in Concrete under Seismic Action

According to Mahrenholtz and Pregartner (2016), even tough anchorages in NSEs represent more than half the volume of designed anchors, they are often neglected in the design process. Anchor qualifications in USA and Europe stretch back until 1975 when the first post-installed anchors were certified. However, these guidelines were limited to static loading until 2001 and 2013, for USA and Europe respectively, when the first amendments were made for the assessment of anchors under seismic loading. While the USA prescribe one performance category for the anchors (ACI 355) the European guideline, EOTA (2013b), prescribes two performance categories: C1 (analogous to the American ACI 355) and C2. As Mahrenholtz and Pregartner (2016) explain, being the demanding requirements for C2 approval more stringent it can be concluded that the European process of qualification is more conservative than the USA one. Nonetheless the selection parameters for C1 vs C2 is still debated in Europe since the recommendations for performance categories do not account for any attenuating effects of seismic response of the building or its ductility on the actions on the anchors.

Testing on fasteners should consider that the behaviour of anchorages during a seismic event is dependent on several parameters. Muciaccia (2017) enlists these factors as:

- The maximum force applied on the fastener;
- The variation of both amplitude and number of cycles of the applied force;
- The maximum crack width of the base material;
- The variation of both amplitude and number of cycles of the crack width.

European Guidelines

In Europe the last revision of ETAG 001 included a new Annex E, EOTA (2013b), dealing with the assessment of metal anchors on concrete under seismic action. As stated before, the evaluation of the performance of anchors subjected to seismic loading is based on two seismic performance categories: C1 and C2, being C2 is more demanding than C1.

1. Performance Category C1 - Anchor capacity is determined in terms of strength (forces). Comprises tests under pulsating tension load and under alternating shear load
2. Performance Category C2 - Anchor capacity is determined in terms of both strength and deformations. Comprises reference tests up to failure and tests under crack cycling as well as the tests included in C1.

In EOTA (2013b) the recommended use of the performance categories is made considering the seismicity and building importance class as it is defined in table 2.4.

Table 2.4: Minimum recommended performance categories for anchors under seismic actions (in EOTA (2013b))

Seismicity		***Importance Class acc. to EN 1998-1:2004, 4.2.5***			
	$a_g \cdot S$ [2)]	***I***	***II***	***III***	***IV***
Very low[1)]	$a_g \cdot S \leq 0{,}05\ g$	*ETAG 001 Part 1 to Part 5*			
Low[1)]	$0{,}05\ g < a_g \cdot S \leq 0{,}1\ g$	*C1*	*C1* [3)] *or C2* [4)]		*C2*
	$a_g \cdot S > 0{,}1\ g$	*C1*	*C2*		

1) *Definition according to EN 1998-1:2004, 3.2.1.*

2) $a_g = \gamma_I \cdot a_{gR}$ *Design ground acceleration on type A ground (Ground types as defined in EN 1998-1:2004, Table 3.1);*
γ_I *= importance factor (see EN 1998-1:2004, 4.2.5);*
a_{gR} *= reference peak ground acceleration on type A ground (see EN 1998-1:2004, 3.2.1);*
S = *Soil factor (see e.g. EN 1998-1:2004, 3.2.2).*

3) *C1 for fixing non-structural elements to structures*

4) *C2 for fixing structural elements to structures*

All the specifications for the test layout, namely test members dimensions, embedment depth, crack control among others is defined in the guideline.

2.5.4 Provision for Façade Systems

In France CSTB, Centre Scientifique et Technique du Bâtiment, issued Cahier 3725 CSTB (2013). This document specifies special provisions for façade systems both in terms of estimation of seismic forces as in terms of experimental testing of façade systems.

Seismic Force Estimation

According to CSTB (2013) a simplified model can be used to compute the global seismic action applied to each fastener in a façade system, single or in a group as (2.25):

$$F_{a_f} = 2.75\gamma_I S a_{gr} m K_{alea} \frac{R_a}{z} \tag{2.25}$$

where the total weight taken up by each anchor, G is computed as (2.26):

$$G = mgK_{alea} \frac{R_a}{z} \tag{2.26}$$

and

$m =$ Mass distributed on the fastener;

$g =$ Gravitic acceleration;

$K_{alea} =$ A coefficient taking into account the uncertainties of distribution of loads due to implementation, equal to 1.5

$\gamma_I =$ Importance factor

$a_{gr} =$ Nominal acceleration at the floor level

$S =$ Soil Parameter

$z =$ Number of fixing points

$R_a =$ Support Reaction coefficient, function of the number of fixing points.

The actions for which the fastener should be design are the combination between $F_{a_{x,f}}$, $F_{a_{y,f}}$ and G. It is important to notice that this prescription is similar to Eurocode 8, CEN (2014), apart from the coefficients K_{alea} and R_a, in other words, these prescription adds to EC8 considerations about the redistribution of forces in fasteners working as a group.

Test protocols

Apart from the prescribed tests in Europe, CSTB, in France, proposed an approach for the study of stability of cladding in seismic zones. The resultant document Cahier 3725 CSTB (2013) describes a test layout for studying the seismic behaviour of anchors involved in these systems. While ETAG 001 prescribes tests to be performed on a single fastener, CSTB exploits the behaviour of a group of fasteners by creating a model on a real scale wall. The purpose of this test is to observe the behaviour of the cladding system when the element to which it is attached is acted in its plane by imposing a cyclic displacement as shown in figure 2.12.

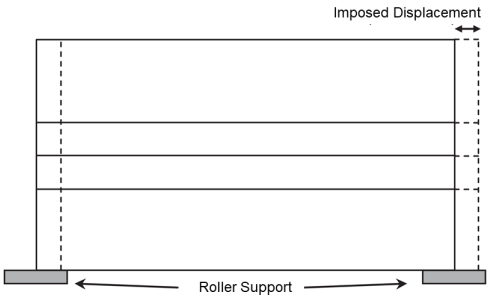

Figure 2.12: Dynamic Test Mechanism (adapted from CSTB (2013))

The dynamic tests are carried out in a test frame designed to test façades with an one direction excitation as shown in figure 2.13. The protocol begins by determining the natural frequency of the system by experimentally applying shock tests. These tests are performed subjecting the structure to a single impulse short enough to allow the structure to promptly reach a stationary state. To determine the eigen frequency six shock tests should be made: three tests with a 2 mm punch plus three tests with a 3 mm punch to evaluate the influence of amplitude of the impulse on the overall response.

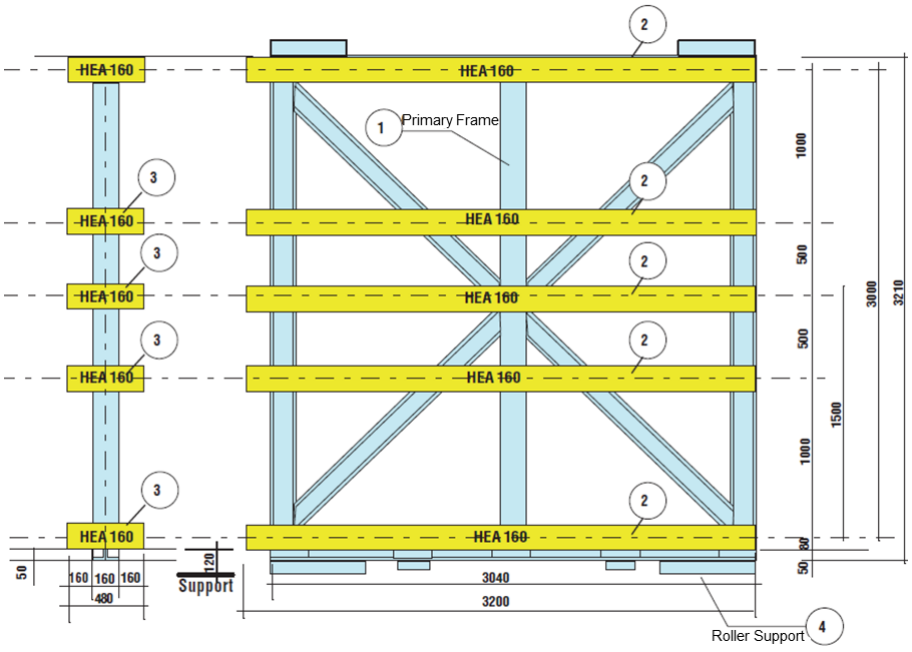

Figure 2.13: Scheme of a Test Frame for application in Dynamic Tests (adapted from CSTB (2013))

Once the natural frequency of the system is known, two different paths should be followed depending on whether this parameter is higher or lower than 15 Hz. For the latest the structure should be tested for its resonant frequency while for the first the normal protocol should be followed. In this test protocol, the model is subjected to 8 successive test phases of increasing acceleration, applied to the wall by means of frequency and displacement amplitude. For each phase three sequences of 20 cycles are performed in ascending order of frequencies as shown in table 2.5. At the end of each phase a pause is made to observe the system's components. The test should stop as soon as there is failure in one of the elements or at the end of the 8^{th} phase.

Table 2.5: Dynamic Test Protocol - Phase description in CSTB (2013)

	Phase 1	Phase 2	Phase 3	Phase 4	Phase 5	Phase 6	Phase 7	Phase 8
	Acceleration $[m/s^2]$							
f [Hz]	3.5	5	6.4	8	9.3	11.2	14	16.5
2	20 cycles	20 cycles	20 cycles	20 cycles				
3					20 cycles	20 cycles	20 cycles	20 cycles
5	20 cycles	20 cycles	20 cycles					
6				20 cycles				
7					20 cycles	20 cycles		
8	20 cycles						20 cycles	20 cycles
9		20 cycles						
10			20 cycles					
11				20 cycles				
12					20 cycles			
13						20 cycles		
14							20 cycles	
15								20 cycles

Loads on Fasteners

Apart from setting the testing protocol as well as an estimation of the horizontal force on the façade, Cahier 3725 CSTB (2013) also explicitly defines how to compute the forces acting on the fastener. It is assumed that the transfer mechanism between the seismic action on the façade and the fastener is through the angle bracket and related to its geometry.

Accordingly, this document prescribes different expressions, depending on the geometry of this angle bracket, to compute the horizontal and vertical force on the fastener for both actions in and out of the façade's plane. As an example the expressions for type 1 angle brackets (represented in figure 2.14) are presented for an in-plane action, where N is the axial force on the fastener (equation 2.27) and V is the shear force (expression 2.28). It is assumed that only two forces are acting on the fastener, the weight, G, and the seismic force $F_{ax,f}$.

$$N = \frac{G/2(l_6 + l_8)}{2/3l_4} + \frac{F_{a_{x,f}}/2(l_6 + l_8)}{2/3l_1} \tag{2.27}$$

$$V = \sqrt{G^2 + {F_{a_{x,f}}}^2} \tag{2.28}$$

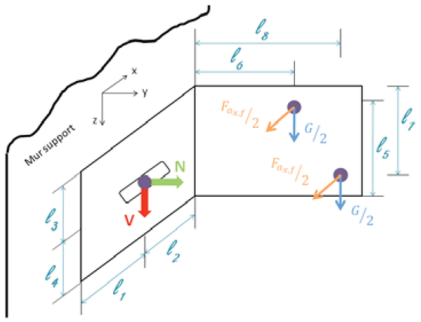

Figure 2.14: Distribution of forces on the angle bracket (in CSTB (2013))

Note that the weight G must consider the distribution of mass through all the fasteners using, for example, the influence area of the fastener. The seismic force should also be distributed through the fasteners. Expression 2.25 already considers the force acting on a single fastener, however if expressions from building codes are used, such as 2.20 or 2.23, the existence of several fasteners must be considered.

Chapter 3

Test Layout

The present document describes an analysis executed with fundamental data that stem from an experimental analysis performed in a collaboration between Politecnico di Milano and CSTB on plastic anchors. The goal of the study was to establish an evaluation method on the resistance of the anchor under seismic loading.

With this goal in mind, static, cyclic and dynamic tests were performed on the anchor based on different test layouts. The tests can be divided into two big groups: the first regards tests on a real scale wall under dynamic loading, while the second consists on tests on a single fastener, both cyclic and static. These experimental results come from a combination between protocols prescribed by CSTB (2013) and alternative protocols developed for this study.

Information about the tested specimen can be obtained on the appendix

3.1 Test Frame

The dynamic tests on a wall were carried out in a layout that involved a cladding composed of several elements, connected to the concrete or masonry wall through six anchors as shown in figure 3.1:

- A bracket ensuring the connection between the wall and a wooden vertical element;
- Wooden supports fixed to the façade element and to the steel brackets. These supports were in epicea timber and presented a section of $65 \times 50mm^2$ and a length of 2.6 m and were fixed to the brackets with one $\phi 10$ and two $\phi 8$ bolts.
- Façade elements with a surface of $0.7 \times 2.6m^2$, TRESPA METEON DUO model, connected to the wooden supports using 5 bolts on each side

According to Politecnico di Milano (2016), the arrangement of angle brackets was designed in order to reduce the uncertainties of transfer mechanism. To this sense, six fixing points were prescribed: four with vertically slotted angle brackets and two with horizontally slotted angle brackets. It is assumed that only the vertically slotted fixtures will transfer seismic load.

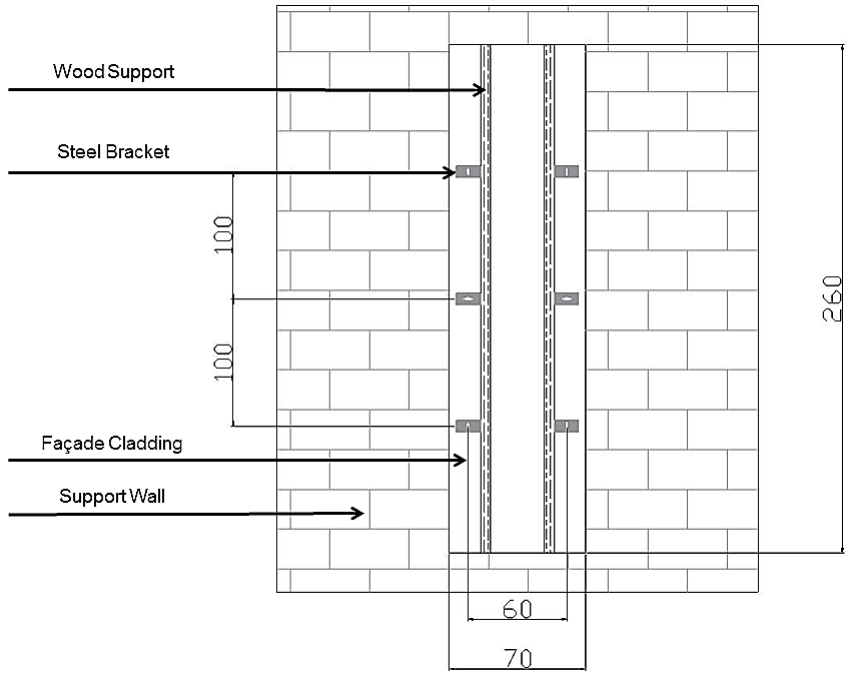

(a) Front view

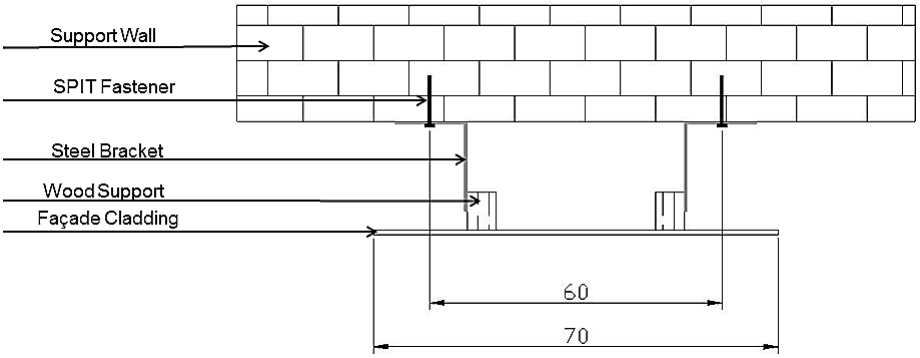

(b) Top view

Figure 3.1: Tested Cladding Layout

3.1.1 Materials

Supporting Wall

Two different supporting walls were used for the dynamic test. First a concrete wall made with C20/25 and later a masonry wall built with Porothon bricks and WEBER mortar. As reported by CSTB (2016), the masonry bricks were tested in compression using 3 repeatability tests. The attained mean resistance is 5.2 MPa, however, a high scatter of results was observed with a variance of around 34%.

Façade Cladding

For these tests several hypothesis of commercial cladding were taken into account, after the preliminary design it was chosen to use TRESPA METEON DUO with a surface of $0.7 \times 2.6m^2$ and an $8mm$ thickness. These cladding were used either in one layer or in a 4 layer combination depending on the test. The main characteristics of this element can be seen in table 3.1.

Table 3.1: Façade Cladding - Mechanical Properties (adapted from Trespa (2012))

	Weight $[kg/m^2]$	**Modulus of Elasticity** **[MPa]**	**Resistance to Fixings** **[N]**
Trespa METEON DUO 8 mm	10.8	$\geqslant 9000$	$\geqslant 3000$

Steel Brackets

For the steel brackets two different models were used. As stated on the technical report, Politecnico di Milano (2016), on the first tests a designed bracket was used (from here forward named ideal bracket), in order to avoid the yielding on the bracket and evaluate the performance of the fasteners on linear elastic behaviour conditions, later, a commercial bracket was introduced in order to assess the behaviour of the anchors in a real configuration scheme. The dimensions of these elements can be seen in figure 3.2

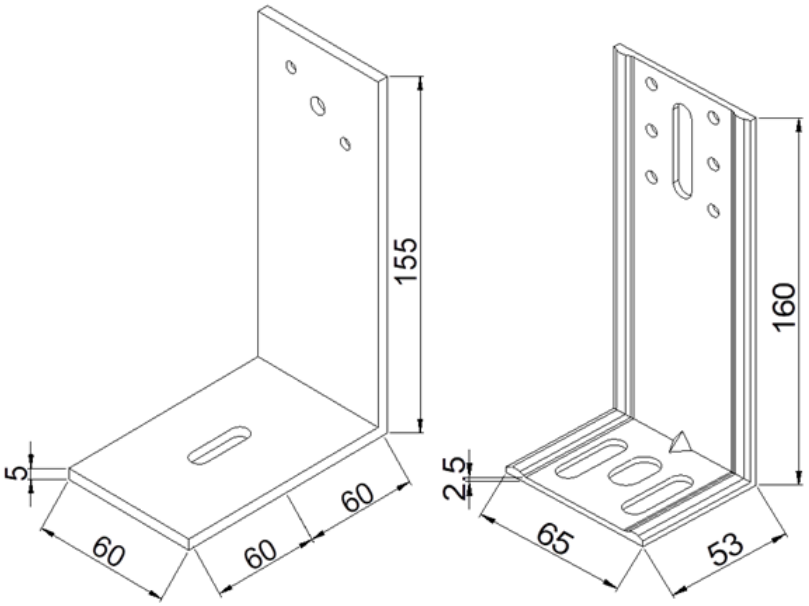

(a) Ideal Angle Bracket (b) Simpson ABC strong tie 160x2.5

Figure 3.2: Brackets Geometry [mm]

For the design of the ideal bracket a simplified model was used in order to estimate the seismic load. Since the amplification of this load is dependent on the eigen frequency of the system then the estimation of this parameter is necessary for the design of the ideal bracket. This simplified model was build as a lumped mass model where the mass of the façade cladding was equally distributed amongst the six fixing point. Additionally, the influence of the façade cladding and wooden supports on the stiffness of the system was taken into account with two limit cases: the former assuming free rotation of the wooden element and the latter assuming totally restrained rotation of this element. On figure 3.3 a scheme of this reasoning can be observed.

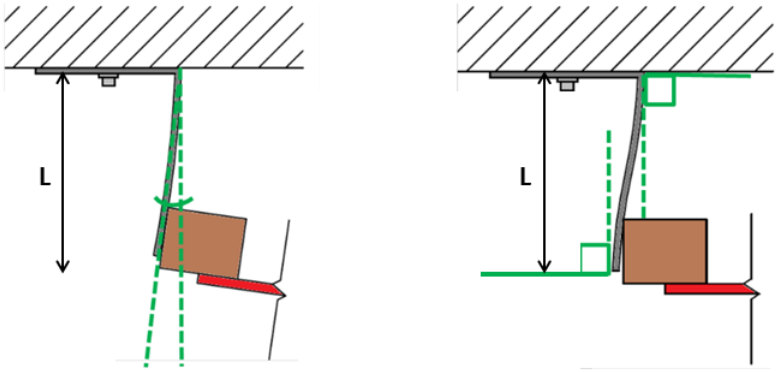

Figure 3.3: Simplified Model for Bracket Design (adapted from Politecnico di Milano (2016))

Table 3.2 compares the main geometric characteristics between the two angle brackets.

Table 3.2: Comparison between designed and commercial steel bracket (in Politecnico di Milano (2016))

Angle Bracket	**Steel**	**Length [mm]**	**Width [mm]**	**Thickness [mm]**
Ideal Angle Bracket	S235	155	125	5
Simpson ABC Strong Tie	Mild Steel	160	65	2.5

It can be seen that the main differences between the ideal and the commercial fastener is the thickness and the length of the flange. The first is related to the fact that yielding of the fastener was to be avoided, in this way, it is ensured an elastic behaviour of the bracket for any value of applied acceleration throughout the frame test. The increase length of the flange of the steel bracket was prescribed in order to reduce the axial force on the fastener, by increasing the lever arm, the resisting moment can be attained with a lower force on the fastener avoiding pull-out failure of this element.

3.1.2 Measurements

Several devices where used to acquire the data used in the analysis of the behaviour of the system. As reported in CSTB (2016), the measured data consisted in displacement and acceleration of the components of both the wall and the façade as well as the forces on the fasteners. The tension force on each fastener was measured through a ring piezoelectric sensor placed at the remaining free length. The wall-ground displacement was measured through an LVDT placed at the bottom of the frame sustaining the wall while the façade-wall displacement is measured at the bottom of the cladding. Next to the LVDT measuring the relative displacement of the cladding an accelerometer allows the measurement of the acceleration of this component while the acceleration on the supporting wall was measured by an accelerometer connected to the bottom of the test frame. Figure 3.4 displays the location of these devices.

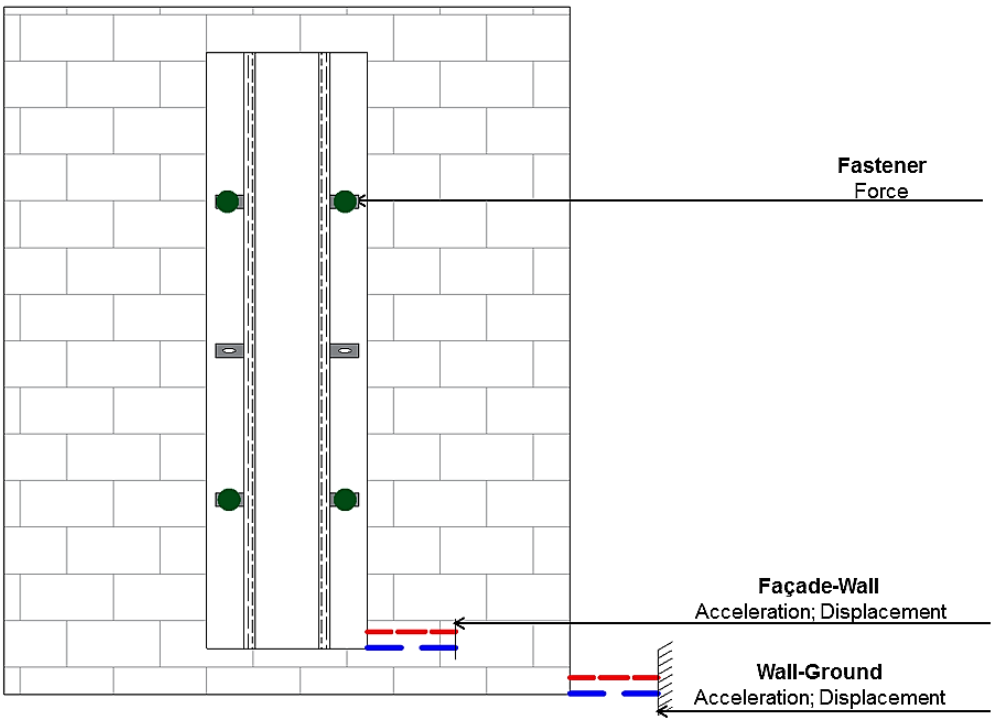

Figure 3.4: Measurements Devices Location

3.1.3 Test Program

In order to assess the behaviour of the fastener distinct tests with different elements were performed. The test program can then be divided into three groups of tests:

1. Tests on concrete wall with ideal brackets;
2. Tests on masonry wall with ideal brackets;
3. Tests on masonry wall with Simpson brackets.

For each group, two tests were performed using a cladding made by one and four panels. In this way it is possible to grasp the influence of mass on a system of this kind. In each test the protocol prescribed by CSTB (2013) for the study of façades under seismic loading was performed. Shock tests were made to obtain the natural frequency of the structure and the dynamic test consisted on the eight phases described on the previous chapter. For some, post-dynamic shock tests where performed as a way of diagnose some damage due to the dynamic loading. The designation for the tests used throughout this document is defined in table 3.3.

Apart from the dynamic tests on the wall also residual tests were made in order to attain the fastener's residual pull out strength as well as its residual stiffness. The wall was positioned horizontally and displacement controlled tests were performed in all 4 anchors while keeping the bracket attached to the anchor.

Because the steel bracket is of importance when analysing the structure, bending tests were performed on both ideal bracket and Simpson Bracket, this allowed the estimation of a deformation curve and consequently the real stiffness of the element. Test layout can be seen in Figures 3.5 and 3.6,

Table 3.3: Designation of Frame tests

Supporting Wall	Steel Bracket	Number of Cladding	Test
Concrete	Ideal Bracket	1	C1_b1
		4	C4_b1
Masonry	Ideal Bracket	1	M1_b1
		4	M4_b1
	Simpson ABC	1	M1_b2
		4	M4_b2

where two different bending directions were tested. For each bracket the load should be applied at the distance where the wooden support transfer the load. According to CSTB (2016) for the ideal bracket the application point is at 132 mm while for Simpson bracket this value is 108 mm as seen in picture 3.5 and 3.6.

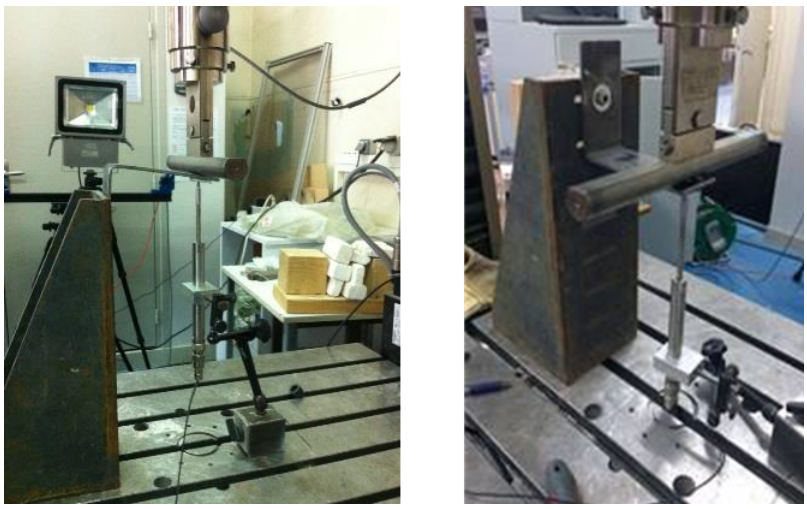

Figure 3.5: Brackets Bending Tests: Ideal Steel Bracket (in CSTB (2016))

Figure 3.6: Brackets Bending Tests: Simpson ABC Bracket (in CSTB (2016))

3.2 Single Fastener

For single fasteners tests were performed both at CSTB and at Laboratorio di Prove Materiali, Strutture e Costruzione (LPMSC) at Politecnico di Milano. The tests on single fastener consisted in static reference tests and cyclic tests. At Politecnico di Milano tests on single fastener's behaviour were made in Porothon Blocks while at CSTB both concrete and masonry were used. The tests performed at each institution are summarized in tables 3.4 and 3.5.

Table 3.4: Designation of CSTB tests on single fastener (in Politecnico di Milano (2016))

Code	Description	Base material
C-S	Static reference test	Concrete
C-01a	Cyclic test Protocol 01a	Concrete
M1-S	Static reference test	Single Poroton block
M1-01a	Cyclic test Protocol 01a	Single Poroton block
M01-01b	Cyclic test Protocol 01b	Single Poroton block
M02-S	Static reference test	Masonry
M02-01a	Cyclic test Protocol 01a	Masonry
M02-01b	Cyclic test Protocol 01b	Masonry

Table 3.5: Designation of PoliMI tests on single fastener (in Politecnico di Milano (2016))

Code	Description	Base material
Mxx-S	Static reference test	Single Porothon block
Mxx-01a	Cyclic test Protocol 01a	Single Porothon block
Mxx-01b	Cyclic test Protocol 01b	Single Porothon block

For each test series, the following parameters are evaluated:

- Mean value of the ultimate tensile load;
- Variance and Coefficient of Variation of the ultimate tensile load;
- Mean value of the displacement at the end of cyclic phase;
- Variance and Coefficient of Variation of the displacement at the end of cyclic phase.

Regarding the cyclic tests, the same loading model used for the shaking table test was used, with 8 phases of 60 cycles each. However, because testing with 15 Hz frequencies may be complex, two test protocols where prescribed, Protocol 01a with a maximum frequency of 15 Hz and Protocol 01b with test's frequency up to 8 Hz. The results were compared at the end of the analysis.

Table 3.6 and table 3.7 describe, respectively, Protocol 01a and 01b, where N_{max} and V_{max} represent the maximum tension force and the maximum shear force prescribed by the manufacturer, and N_i and V_i represent the load acting on each phase.

Table 3.6: Phase description - Protocol 01a (adapted from Politecnico di Milano (2016))

	a $[m/s^2]$	N_i/N_{max}	**f** **[Hz]**	n_{cycles}
			2	20
Phase 1	3.5	0.2	5	20
			8	20
			2	20
Phase 2	5	0.3	5	20
			9	20
			2	20
Phase 3	6.4	0.4	5	20
			10	20
			2	20
Phase 4	8	0.5	5	20
			11	20
			3	20
Phase 5	9.3	0.55	7	20
			12	20
			3	20
Phase 6	11.2	0.7	7	20
			13	20
			3	20
Phase 7	14	0.85	8	20
			14	20
			3	20
Phase 8	16.5	1	8	20
			15	20

Table 3.7: Phase description - Protocol 01b (adapted from Politecnico di Milano (2016))

	a $[m/s^2]$	N_i/N_{max}	**f** **[Hz]**	n_{cycles}
Phase 1	3.5	0.2	2	20
			5	40
Phase 2	5	0.3	2	20
			5	40
Phase 3	6.4	0.4	2	20
			5	40
Phase 4	8	0.5	2	20
			5	40
Phase 5	9.3	0.55	3	20
			7	40
Phase 6	11.2	0.7	3	20
			7	40
Phase 7	14	0.85	3	20
			8	40
Phase 8	16.5	1	3	20
			8	40

Chapter 4

Test Results

4.1 Test Frame

As stated before, one of the results from the tests performed on a real scale wall was the axial force on fasteners. In order to analyse these results the fasteners were numbered according to figure 4.1. This reference is used on the analysis presented throughout the following sections.

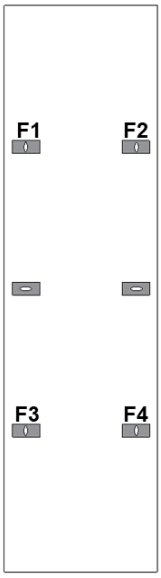

Figure 4.1: Numbering of Studied Fasteners

4.1.1 Steel Bracket Bending Test

As stated in the previous chapter, bending tests were performed in order to assess the parameters related to these element's behaviour. Force-displacement curves were plotted as shown in figures 4.2 and 4.3.

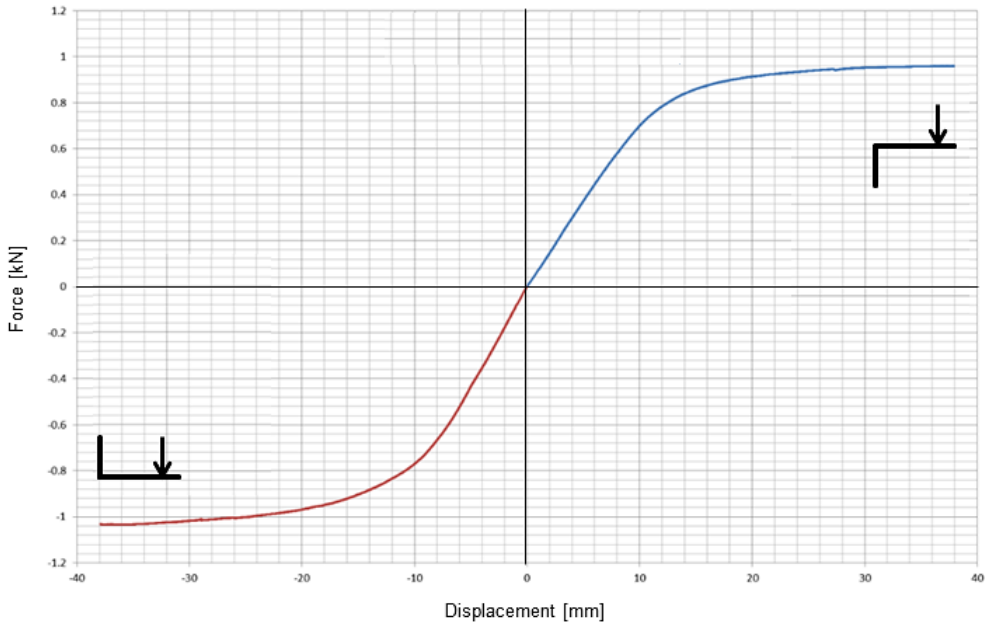

Figure 4.2: Load-Displacement Curve - Bending Test on Ideal Steel Bracket (adapted from CSTB (2016))

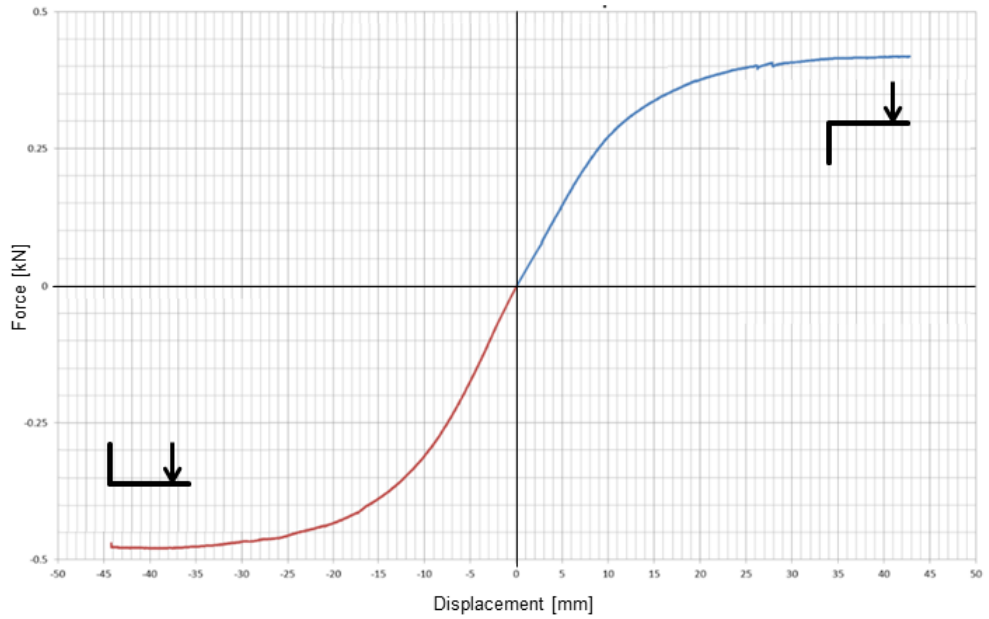

Figure 4.3: Load-Displacement Curve - Bending Test on Simpson ABC Bracket (adapted from CSTB (2016))

Both the stiffness of the fastener and the yielding force can be estimated from these curves. For the ideal bracket, the stiffness is close to 0.07 kN/mm and the yielding plateau is near 1 kN in both directions, while for SIMPSON ABC bracket, the stiffness is close to 0.03 kN/mm and the yielding plateau is near 0.4 kN and 0.5 kN.

4.1.2 Shock Tests

Shock Tests work as an horizontal impulse to the structure allowing an observation of its behaviour under free vibration. This impulse is done by imposing a fast displacement to the wall, with variable magnitude, returning this element to the initial configuration. This will induce an acceleration to the cladding leading to vibrations even after the supporting structure stop moving. For the tests performed on the test frame, this displacement is in-plane with the supporting wall.

An example of a shock test's time-displacement plot is can be seen in figure 4.4. Notice that after a short initial transient state it is possible to identify the system's steady state response.

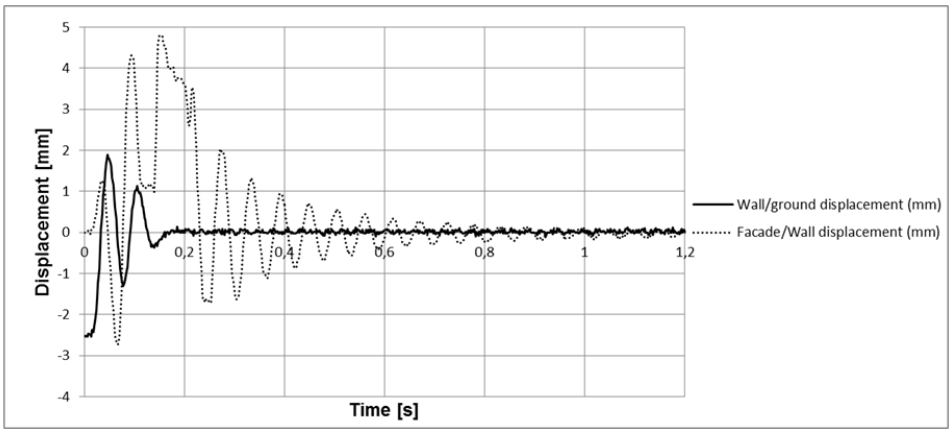

Figure 4.4: 2 mm Shock Test for Masonry Wall with Ideal Bracket Dynamic Test

Eigen Frequency

As stated before, CSTB protocol for façade tests begins with shock tests that allow an estimation of the natural frequency of the system. Results from these tests where analysed by CSTB and Politecnico di Milano, having the Fourier transform of the gathered data as the basis for this computation. The results from this analysis can be seen in table 4.1.

Table 4.1: Computed Eigen Frequency from Shock Tests (in CSTB (2016))

Test	Cladding	Eigen Frequency $[Hz]$
C1_b1	1	29.3
C4_b1	4	16.8
M1_b1	1	31.8
M4_b1	4	30.7
M1_b2	1	19.3
M4_b2	4	18.7

Since these results come from an in-plane impulse, the presented frequency is the natural frequency of the system associated with the first vibration mode.

Damping Ratio

Besides the natural frequency of the system, also the damping factor can be computed from the shock test results. These tests allow the system to reach steady state conditions. As a result it is possible from the displacement-time plots, using the logarithmic decrement method, to compute this parameter. The results for concrete wall tests are summarized in table 4.2.

Table 4.2: Damping Ratios obtained through Logarithmic Decrement

Test	Number of Cladding	Shock Test						Average
		2 mm			3 mm			
C_b1	**1**	0.050	0.058	0.056	0.064	0.080	0.094	**0.067**
	4	0.055	0.058	0.060	0.122	0.084	0.085	**0.077**
M_b1	**1**	0.028	0.037	0.021	0.014	0.032	0.034	**0.028**
	4	0.051	0.043	0.043	0.037	0.037	0.040	**0.042**
M_b2	**1**	0.022	0.052	0.038	0.041	0.020	0.035	**0.035**
	4	0.034	0.056	0.057	0.051	0.039	0.042	**0.047**

It is possible to notice that for higher mass systems higher damping ratios are attained, in other words, higher mass systems are favourable to energy dissipation, which may indicate a frictional damping mechanism. Moreover, as expected, this damping ratio is lower on masonry that in concrete.

It can be observed that in C4_b1, a 3 mm shock leads to higher damping ratios than the 2 mm shock. Since in the other tests it can be observed that the system's damping is rate-independent, it is expected that this difference shouldn't arise from the variation of the impulse's velocity.

However, for the same time interval, a 3 mm impulse induces a higher acceleration than a 2 mm impulse, in this sense, small damages or sliding of the bracket may lead to a higher dissipation of energy, hence, a higher damping ratio. In figure 4.5 it is possible to compare the two wall displacement impulses for the dynamic test on concrete wall with 4 cladding. It is easily observed that the the time interval is similar for both actions, this means that for the higher displacement the system is subjected to a much higher acceleration. Also, the biggest impulse is in reality greater than the prescribed 3 mm.

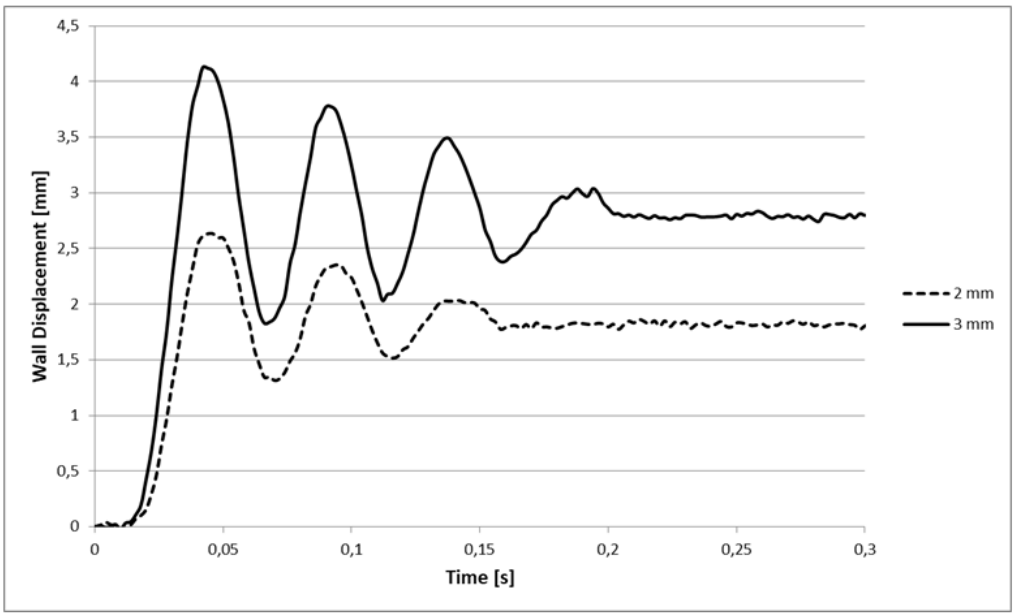

Figure 4.5: Comparison of Shock Tests on Concrete wall with 4 Claddings

4.1.3 Dynamic Tests

As previously stated three cyclic tests were performed on the framed wall. The results were obtained in terms of displacement, accelerations and forces on the fasteners. In this section a closer look to the loading on fasteners is made. Specifically on the relation between the theoretical formulation and the real forces on fasteners.

The theoretical values on the forces can be estimated with CSTB's prescription 2.27, however this formulation is over conservative and so, the theoretical values can be computed assuming a rigid bracket with linear distribution of forces. In this way the axial load on the fastener can simply be estimated according to expression 4.1.

$$N = \frac{G \cdot a}{c} + \frac{F_{a_{x,f}} \cdot a}{b} \tag{4.1}$$

where,

N is the axial force on the fastener;

G is the weight acting on the fastener;

$F_{a_{x,f}}$ is the estimated seismic force acting on the structure;

a, b, c are geometrical properties of the bracket as shown in figure 4.6.

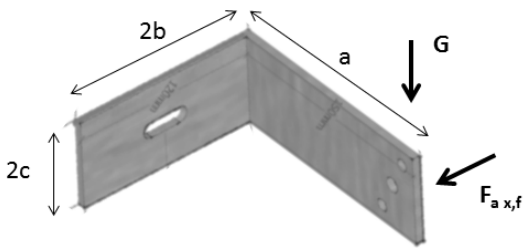

Figure 4.6: Bracket's Geometry

The theoretical estimation for the forces on fasteners can be obtained using both CSTB and Eurocode 8 prescriptions. The main difference between the two analysis is that, as stated before, CSTB assumes a constant amplification factor equal to 2.75, while the amplification assumed in Eurocode is dependent on the relation between the action's frequency and the natural frequency of the structure. This amplification can be estimated according to equation 4.2.

$$G_{EC8} = 2A_{EC8} - 0.5 \tag{4.2}$$

where,

$$A_{EC8} = \frac{3}{1 + \left(1 - \frac{f_1}{f_a}\right)^2} \tag{4.3}$$

In expression 4.3, f_a represents the natural frequency resulting from the shock tests while f_1 represents the action's frequency, in this case taken as the maximum frequency from each phase. With this in mind it is possible to compare the results from both formulations. The comparison plot can be seen in appendix.

It is possible to understand that considering a constant amplification factor may underestimate the forces acting on the fasteners, while Eurocode 8 proposition is more similar to the real forces acting on the anchors.

With the previous considerations in mind, it is possible to relate the force acting on the fasteners with the acceleration of the wall, the mass of the façade system and the natural frequency of the system. Consequently, it is possible to arrive to the expected theoretical values for the seismic force, computed for each phase according to expression 4.4.

$$F_{a_{x,f}} = G_{EC8} \times a \times m \tag{4.4}$$

where a is the imposed wall acceleration and m is the system's mass.

According to CSTB (2013) the expected force on the fastener should take into account uncertainties on the distribution of forces due to fastener's installation and displacements, this is attained through the coefficient K_{alea} that considers a maximum redistribution of 50%. In this way, an upper and lower boundary can be obtained for the predicted forces on the fasteners related to the redistribution of forces on these elements.

Using the presented reasoning it is possible to attain the theoretical expected values as shown in appendix.

It is important to notice that, for the 4 cladding test with commercial brackets on masonry wall, yielding of the bracket is expected. In this situation, the dynamic load will no longer be transferred to the anchors and so, the maximum force acting on the fasteners will be the one computed for the resistance of the bracket. In this sense, the limit can be computed as shown in expression 4.5.

$$F_{fast,max} = \frac{M_r}{b} = 1.33kN \tag{4.5}$$

Subsequently to these results it is possible to analyse the empiric values obtained from the tests on real scale wall. For the maximum force computation in each fastener expression 4.6 was used. In this way, since in reality a variation of force is considered, the self weight contribution is cancelled allowing a pure analysis of seismic forces.

$$F_{fastener} = \Delta F = F_{max} - F_{min} \tag{4.6}$$

Concrete Wall with Ideal Angle Brackets

The results obtained from tests on concrete wall with ideal angle brackets can be seen in appendix for both one and four cladding. The tests on concrete wall can be used as a reference test to better understand the behaviour of the façade system since this base material is generally more consistent than masonry.

It can be seen that the experimental results are consistent with the theoretical boundaries and with the linear development of forces with increasing acceleration. Furthermore, it also explicitly shows the redistribution of forces among the fastener's acting as a group.

However in the four cladding test it is possible to remark that the highest load does not occur for the last phase with the highest acceleration. In fact, the peak load is developed in phase 6 for an acceleration of $11.2m/s^2$ while for the higher phases the load remains approximately constant. These results may indicate a non-linear behaviour of the system after the peak phase.

Masonry Wall with Ideal Angle Brackets

The second test to be performed consisted on a Masonry wall with ideal brackets. The layout presented in this tests was, as stated before, designed to prevent bracket failure through the extension of the bracket flange and the increase if this element's thickness. Consequently only the fasteners failure was studied. The results presented in appendix.

From one cladding testing it is perceptible that the scattering of measured forces on fasteners is more significant in this case. It can be related to the fact that since the base material has a higher variability also the performance of fasteners has a bigger discrepancy. Nonetheless, the results are also compatible with the theoretical predictions.

Regarding the test with additional mass, 4 cladding, it can be observed that it was not performed until the limit acceleration. In fact, it was interrupted before the end of the test protocol, this had to do with the fact that, during phase 6, failure of part of the anchoring system was observed. Not only fastener 2 was completely detached from the masonry wall but also fastener 4 suffered a pull-out failure and, even though it did not completely detach from the wall, it could be removed simply by hand with a residual load close to zero.

Subsequently it is clear that for the previous analysed experimental testing, out-of-plane motions had a considerable influence on the behaviour of the façade system. Thus, higher modes of vibration of the system, namely out-of-plane displacements, may have had an important role on the anchorage failure.

Masonry Wall with Commercial Angle Brackets

The final test was designed to evaluate the behaviour of the system under real conditions, consequently, a commercial bracket was used. According to the bending test results on this element, its capacity is lower than the ideal bracket, hence it is expected yielding to take place. The results from test with one cladding are similar to the previously attained for concrete. However for the higher mass system failure of the angle bracket occurs. When the elements leave their elastic range the linear formulation is no longer applicable, instead, it can be seen that loads on fasteners remain approximately constant creating a plateau on the plotted data. In this sense, for this real configuration system, failure will not depend on the capacity of the fasteners but on the capacity of the angle brackets. Nevertheless the upper and lower limits for force redistribution can still be taken into consideration.

4.1.4 Post-Dynamic Shock Tests

For some of the previously listed test configurations, post-dynamic shock tests were performed. In this way it was possible to estimate the eigen frequency after the dynamic loading in order to analyse a possible change in the structure's stiffness and consequently the damaged imposed by this dynamic loading.

Note that since on masonry wall with four cladding failure was observed, namely fastener pull-out with ideal brackets and yielding of the angle bracket with Simpson brackets, the post-dynamic test was not performed. In these tests the existence of structural damage could be evaluated by simple observation. The results from these tests can be observed on table 4.3.

Table 4.3: Computed Eigen Frequency from Post-Dynamic Shock Tests (in CSTB (2016))

Test	**Eigen Frequency [Hz]**	
	Initial	**Post-Dynamic**
C1_b1	29.3	29.7
C4_b1	16.8	17.0
M1_b1	31.8	36.8

From the previous results it can be concluded that, in the analysed dynamic tests no significant damage of the structure occurred in view of the fact that there is no decrease in the system's natural frequency and consequently no decline of its stiffness. It is interesting however to interpret the results obtained for masonry test M1_b1. Not only there was no structural damage but, according to the system's eigen frequency, an increase of stiffness took place.

4.2 Single Fastener

As stated previously, for single fastener testing both static reference and cyclic tests were performed. However, for the scope of this analysis, only static reference tests will be evaluated in order to define

crucial parameters to characterize the fastener's behaviour. The results from these tests can be seen in the appendix.

4.2.1 Static Tests

Reference static tests were performed on single fasteners. Through these tests it is possible to estimate both the initial tangent stiffness of the fastener and its ultimate tensile force under a static load for the two base materials used in the framed wall test, concrete and masonry. The considered range of results was consistent with small displacements, thus, the initial tangent stiffness was computed additionally to the fastener's capacity.

4.2.2 Residual Tests

In order to assess the influence of dynamic loading on the fastener, residual tests were performed on single fasteners after the test frame protocol. These results can be compared with the static reference tests, allowing an understanding of the damage due to dynamic loading of these elements.

From these tests it was possible to attain the residual stiffness of the four installed fasteners, parameter that may be compared with the initial stiffness obtained from the single fastener testing protocols.

Note that since there was fastener's failure by pull out on test on masonry with ideal brackets only the remaining fasteners where tested. All the computations where done assuming small displacements of the fastener, and therefore the initial tangent stiffness was taken into account.

4.2.3 Effect of Dynamic Loading

It is possible to partially understand the effect of the dynamic load on the fasteners comparing the results from the static tests with the residual tests. The static reference values for masonry were taken as the average between Politecnico di Milano and CSTB's results.

The effect of dynamic load is clearer for concrete tests, in fact, even tough only a small decrease in capacity is detected, the initial stiffness is greatly diminished. Analogously for Masonry there is a negligible variation on the fastener's capacity but also a considerable decrease on the initial stiffness.

Chapter 5

Dynamic Analysis

5.1 Simplified Dynamic Models

5.1.1 Natural Frequency of the System

The previously described problem can be studied using a simplified one degree of freedom dynamic model in order to assess the behaviour of the system tested in CSTB. The dynamic analysis of the simplified model was based on several hypothesis.

1. Rigid Supporting Wall;
2. Rigid Façade Panel;
3. Elastic behaviour of the Steel Brackets;
4. Elastic Behaviour of the Fastener;
5. Uniform Distribution of Mass on the Cladding;
6. Negligible Damping.

With these considerations in mind a 2D single degree of freedom system was studied. This model was designed to represent two of the four fasteners assuming that the mass was equally distributed amongst all fasteners and therefore using a tributary area which is equal to half of the façade system as represented in 5.1.

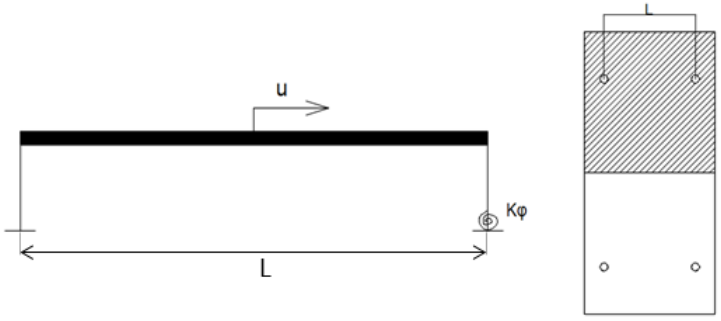

Figure 5.1: Definition of the Model and Tributary Area

A lumped mass discretization was used, assuming the mass of the system to be concentrated only on the façade cladding. This discretization method was chosen since this element represents a minimum of 70% of the total system's mass. Moreover, since tests on framed wall were performed only in the horizontal direction, the horizontal displacement of the cladding was defined as the degree of freedom of the model - u.

The system's behaviour was defined assuming that the action of the bolts can be portrait as a rotational spring at the bottom of the angle brackets, this fictional spring stiffness is obviously dependent on the axial stiffness of the fastener according to the following scheme:

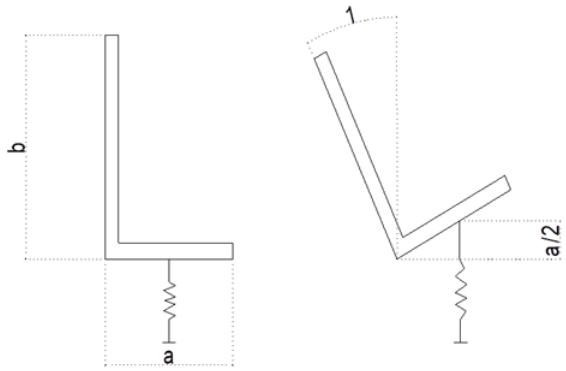

Figure 5.2: Estimation of the Rotational Stiffness of the Spring

Therefore, the relation between the axial stiffness and rotational stiffness can be written as shown in expression 5.1, where k_φ is the rotational stiffness of the fictional spring and k_{fast} is the axial stiffness of the fastener obtained through the static reference tests.

$$K_\varphi = k_{fast} \cdot \left(\frac{a}{2}\right)^2 \tag{5.1}$$

Additionally, to correctly represent the model's stiffness, the stiffness of the angle brackets can be computed based on the bending tests performed at CSTB assuming that the panel constrains the bracket. Hence, the results from the bending tests were assumed to portrait a cantilever scheme while the reference value for the analysis was computed as a double clamped bracket through equation 5.2.

$$K_b{}^{model} = 4K_b{}^{test} \cdot b \tag{5.2}$$

Since the primary goal of this one degree of freedom system's analysis was to compute the natural frequency of the system, it was performed assuming free vibration and that the damping of the system would not lead to significant differences in these values. This hypothesis is in agreement with the damping coefficients range obtained through the shock tests. Hence the equation of motion can be written as 5.3.

$$m\ddot{u} + ku = 0 \tag{5.3}$$

For undamped one degree of freedom systems, the natural frequency can be estimated based only

on the mass and stiffness of the system as shown on the expression 5.4.

$$f_1 = \frac{1}{2\pi}\sqrt{\frac{k}{m}} \tag{5.4}$$

Where the stiffness coefficients were computed using the force method as shown in figure 5.3. With resulting stiffness coefficients expressed in equations 5.5.

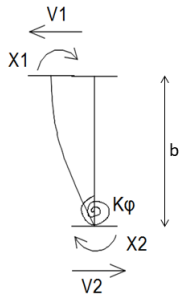

Figure 5.3: Stiffness Coefficients

$$V_1 = V_2 = \frac{3EI}{b^3} + \frac{3}{\frac{b^3}{3EI} + \frac{4b^2}{3k_\varphi}} \tag{5.5a}$$

$$X_1 = \frac{3EI}{b^2} + \frac{1}{\frac{b^2}{3EI} + \frac{4b}{3k_\varphi}} \tag{5.5b}$$

$$X_2 = \frac{1}{\frac{b^2}{6EI} + \frac{2b}{3k_\varphi}} \tag{5.5c}$$

Hence, considering the previous results, the stiffness of the system associated with the studied degree of freedom can be expressed as equation 5.6. Note that a rigid connection between the steel bracket and the wood element is assumed. However, according to the studies performed by Izzi et al. (2016) the stiffness of the steel-wood connection is higher than the bending bracket stiffness, leading to a negligible deformation when compared to the one sustained by the steel bracket.

$$k = k_b + V_1 = k_b \left(\frac{5}{4} + \frac{3}{4 + \frac{4b^2}{3}\frac{k_b}{K_\varphi}} \right) \tag{5.6}$$

Once the stiffness parameter is known, the natural frequency of the system can be attained simply by computing its mass, considering the tributary area, as $m = 2m_{bracket} + m_{facade} + m_{wood}$. In the present case four different values can be estimated depending on the number of cladding and on the type of angle bracket used in the test to be analysed. In table 5.1 these values are summarized for the tributary area previously defined.

Table 5.1: Simplified Model's Mass [kg]

	Number of Cladding	
	1	**4**
Ideal Steel Bracket	14.88	44.36
Simpson ABC Bracket	14.16	43.64

In order to evaluate the results of the model a non-dimensional analysis was made where the non--dimensional frequency was obtained as the ratio of the limit frequency obtained for a zero stiffness of the spring ($f_{1_{Min}}$ in equation 5.7) and the normalised stiffness as a ratio between the stiffness of the fastener and the one from the bracket.

$$f_{1_{Min}} = \frac{1}{2\pi}\sqrt{\frac{k_{min}}{m}} \quad with \quad k_{min} = \frac{5}{4}k_b \tag{5.7}$$

The minimum stiffness, k_{min}, can be attained from expression 5.6 assuming k_φ to be zero. Situation represented by a hinged support.

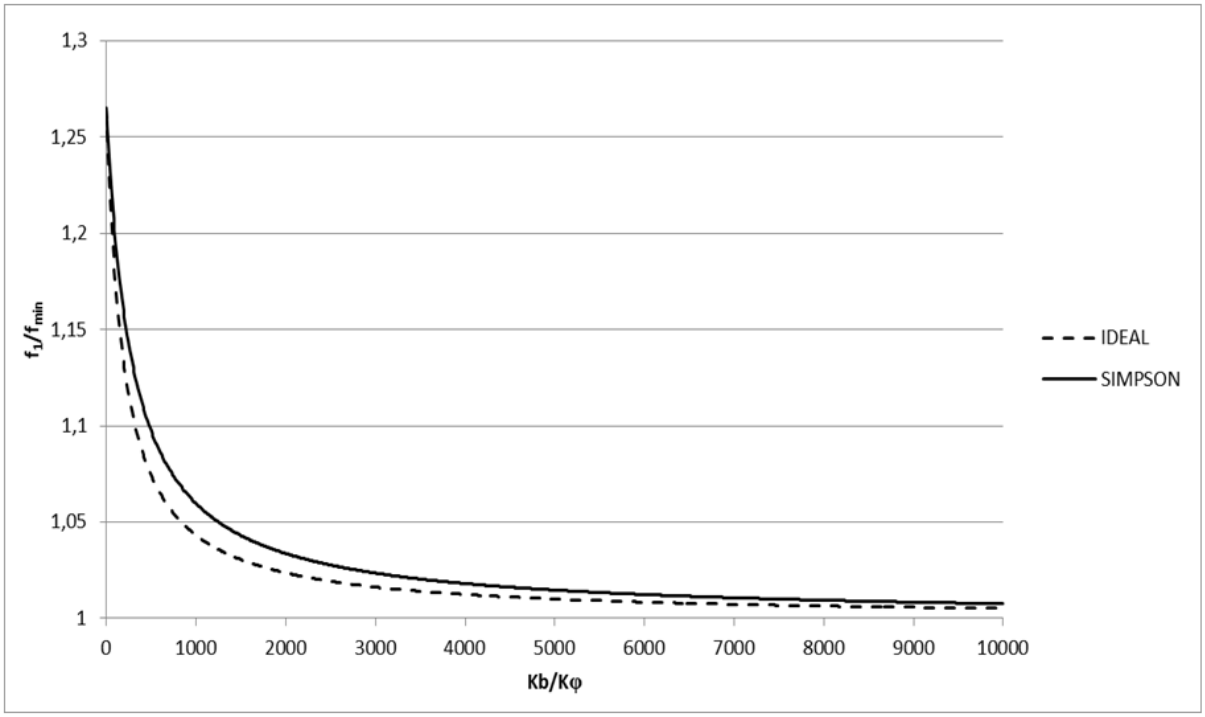

Figure 5.4: Relation between Natural Frequency and Stiffness of the system

In this sense, it is possible to evaluate the sensitivity of the system to the ratio between the stiffness of the brackets and the stiffness of the fastener. From the plot shown (figure 5.4) it can be observer that as expected the system is more sensitive to the fastener's stiffness if it is closer to the order of magnitude of the latest. Moreover it can be seen in figure 5.4, through the asymptotic behaviour tending to the unit, that as expected the limit when the spring's stiffness (k_φ) goes to zero is the one obtained with a hinged support while the expect natural frequency for an infinite rotational spring is the one obtained for

a double clamped angle bracket.

Being that the natural frequency of the system changes with the fastener's stiffness it might be important to pose the question of whether after performing CSTB's protocol on a test frame there is any change on the behaviour of the system, namely on its eigen frequency. In fact, residual tests on the fasteners show a lower axial stiffness then the ones performed before the dynamic excitation. In that sense the data from the axial tests can be used to compute the initial and residual stiffness of the bolts.

In order to study this behaviour, a relation between the residual axial stiffness and the initial axial stiffness can be found and the previous plotted function can be used to estimate the natural frequency. These results are presented in table 5.2. Where k_b is the bracket's stiffness, k_i is the initial stiffness and k_{res} the residual stiffness.

Table 5.2: Natural Frequency Estimation - Pre and Post Dynamic Tests

Test	K_b/K_i	f_1/f_{min}	K_b/K_{res}	f_1/f_{min}
C01	0.3%	1.2649	4.6%	1.2648
M01	1.9%	1.2649	5.3%	1.2648
M02	0.8%	1.2649	2.7%	1.2649

From the data analysed in the previous table it is possible to notice that, on the range studied, the loss of stiffness due to dynamic loading does not influence significantly the natural frequency of the structure, as shown in figure 5.5.

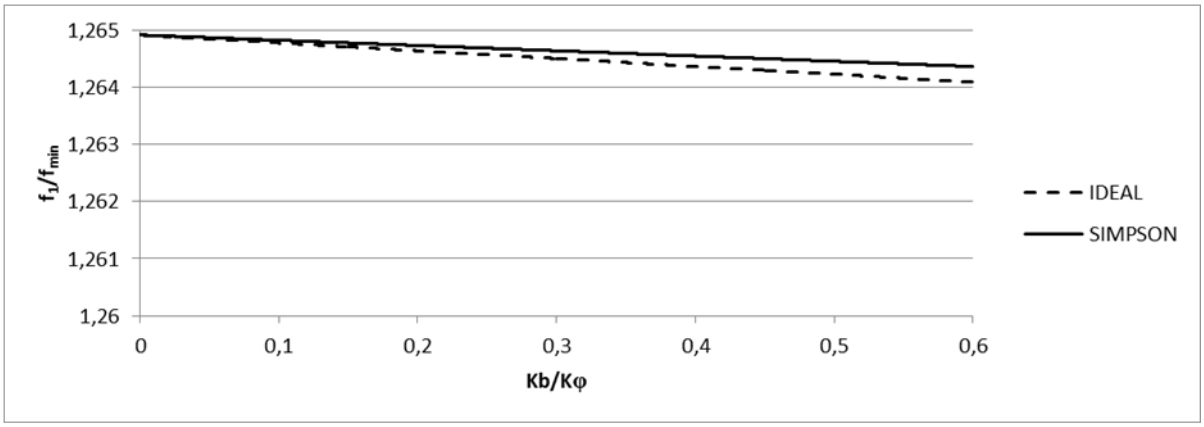

Figure 5.5: Relation between Natural Frequency and Stiffness of the system - Experimental Range

These results are in agreement with the Post-Dynamic shock tests, that demonstrate that the natural frequency of the system is identical before and after the test frame dynamic tests.

5.1.2 Redistribution of the Forces on the Fasteners

The European seismic code, Eurocode 8 CEN (2014), does not explicitly reference the used anchors. Being that the only provisions concerns the seismic force acting on the non-structural element, there is no distinction on whether the fasteners are working in a group or alone, consequently it does not explicitly

states the fact that, when implementing a fastener in a group, there is some uncertainty regarding the distribution of loads. Cahier 3725 CSTB (2013) however, defines two coefficients to account for this issue, as shown in expression 2.25 - R_a to account for the number of fixing points and K_{alea} for the uncertainties of load distribution, both depending on the number of anchors on the system.

To this matter, a model can be built in order to understand the influence of loss of stiffness in one fastener on the distribution of forces on the fixings, being the limit situation the pull out failure of one of the fasteners. In this sense it is possible to understand the range in which the factor of $K_{alea} = 1.5$ is valid.

An analogous dynamic model was built to the one presented at the beginning of this chapter, however, both fixing points were assumed as a rotational spring as shown in figure 5.6. Being their stiffness related to the axial stiffness of the fasteners as presented for the one spring model in expression 5.1.

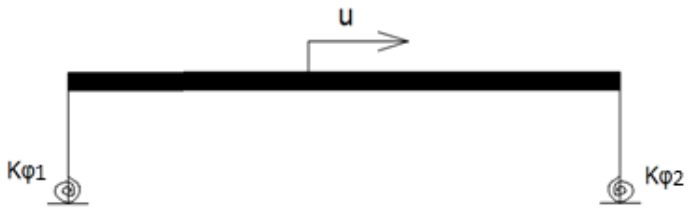

Figure 5.6: Model with 2 rotational Springs

Following this reasoning, it is possible to relate the ratio between force on fastener 1, F_1, with the force on fastener 2, F_2, with the ratio between their stiffness, k_1 and k_2. The results are expressed in graph 5.7.

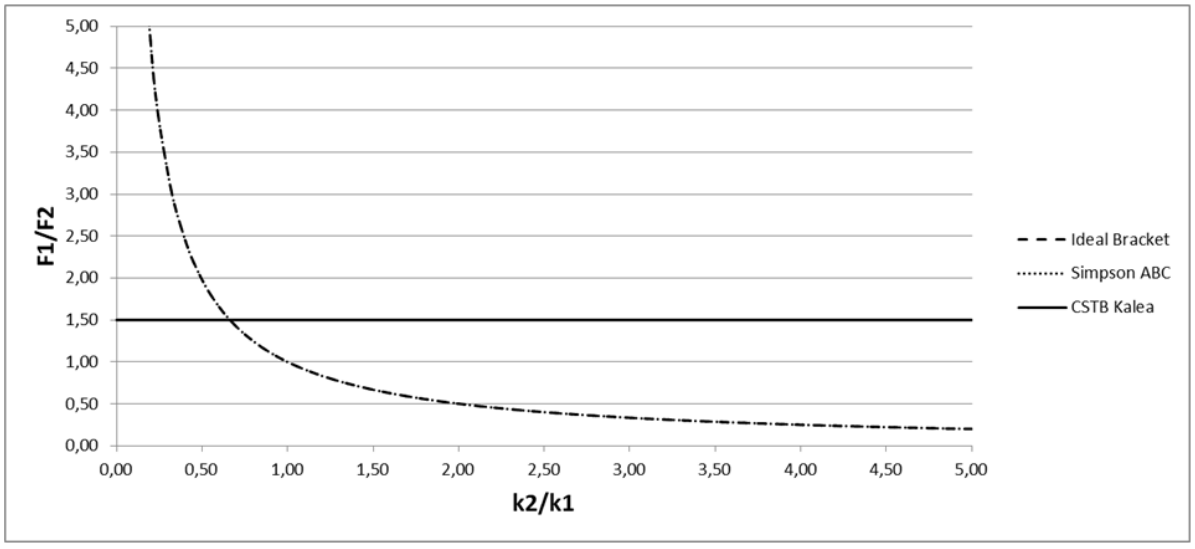

Figure 5.7: Estimation of redistribution Factor

In the results it is possible to observe that the redistribution factor K_{alea} is valid until a stiffness ratio of approximately 65%. It may also be opportune to understand if, on the range in which CSTB's prescribed K_{alea} prameter is valid, the natural frequency of the system may change with this redistribution. In other words, the eigen frequency of the system was studied for the range $k_2 = k_1$ to $k_2 = 0.65k_1$.

The results can be seen in the plot 5.8. Where f_{ref} is the natural frequency obtained for $k_2 = k_1$, the situation where no redistribution occurs.

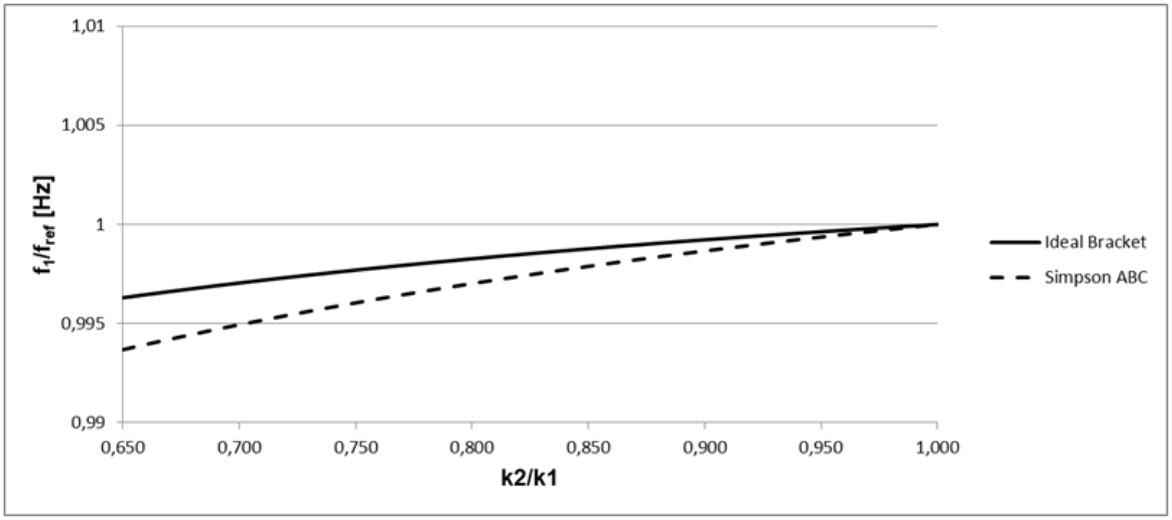

Figure 5.8: Natural Frequency for Redistribution Factor bellow 1.5

An analysis of these results can lead to the conclusion that in this range, redistribution of forces has a negligible influence on the structure's eigen frequency, lower than 1%, in other words a negligible effect on the overall stiffness of the system. Hence, it can be stated that even tough different fasteners stiffness have a considerable influence in the forces acting on the anchor, force redistribution in a practical range has no effect on the natural frequency of the system.

The coefficients obtained for the redistribution of forces on fasteners based on the simplified model can be compared with the experimental ones by considering the stiffness attained from the residual tests performed after the dynamic loading. This parameter will allow the determination of the experimental stiffness ratio, while the measurements on the piezometers during the dynamic test will enable the evaluation of force ratio between fasteners.

A comparison between the theoretical results collected through the simplified dynamic model and the experimental ones for the last phase of the dynamic test in concrete with 4 cladding was attained. This phase was chosen for being the one closer to the residual tests. The results can be seen in appendix.

Being that the development of the simplified model assumes an elastic behaviour of its elements, it does not represent the behaviour of the structure when failure of bracket or anchors occurs. Hence, results attained from tests on masonry are not viable for the analysis performed with tests on concrete wall.

As an important remark, for this simplified model analysis the computation of the ratios should be done between a pair of top fasteners or bottom fasteners, owing to the fact that the dynamic model considers a purely horizontal redistribution. This hypothesis is, however, in agreement with experimental results.

5.2 Transfer Function

As seen, the design force for the connections between structural and non-structural elements is based on the relative acceleration at the level of the connection between the non-structural element and its supporting structure. For the performed dynamic tests, while the acceleration at the structural element is known, as the input acceleration, the acceleration on the façade panel is dependent on its characteristics such as mass and stiffness. Following this reasoning, a relation between the imposed acceleration and the relative acceleration on this element can be found. This relative acceleration can be computed simply by subtracting from the values obtained on the accelerometer attached to the façade panel, the values read by the accelerometer on the wall.

The previously stated relation can be seen as the study of the acceleration amplification between the two elements and so, a transfer function for the different test layouts can be computed. This function describes the frequency response of the system and can be computed using different analysis tools. Because the analysis gathers data in the time domain the Fourier transform can be used in order to have an analysis on frequency domain. Moreover, since the gathered data is discrete the discrete Fourier transform should be computed.

The analysis of the transfer function allows the identification of the eigen frequencies of the system. When analysing these results it was clear that for a range of frequencies inside the scope of this study two modes of vibration were distinguished, being the simplified model described in the previous sub-chapter related to the first one. In figure 5.9 and 5.10 it can be seen an example of the transfer function for the shock tests on concrete wall with ideal angle brackets supporting one and four cladding. An average transfer function was computed between the six functions obtained from these tests. For the remaining test layouts, results can be seen in appendix.

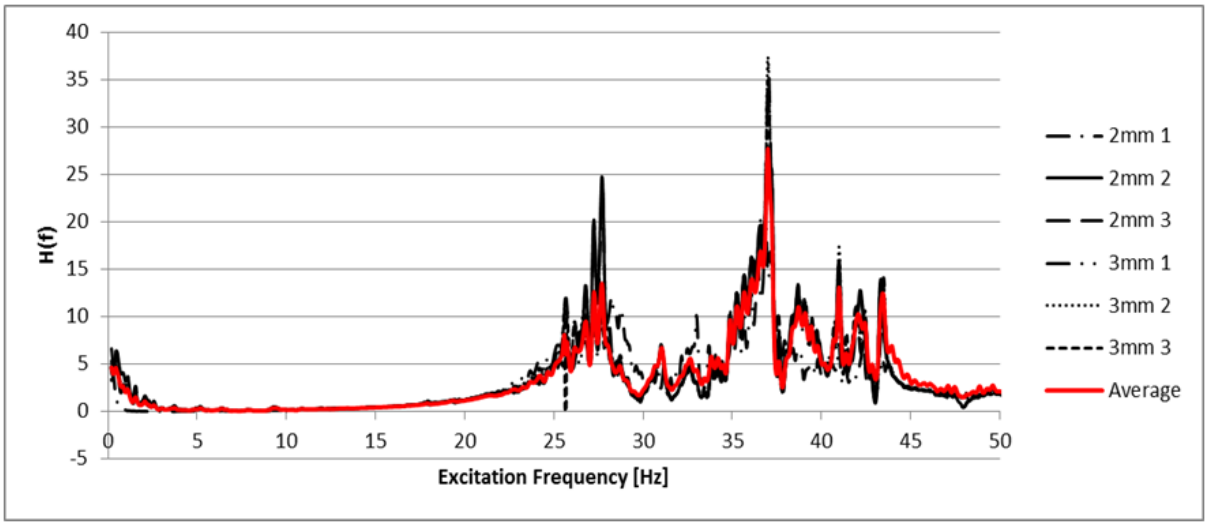

Figure 5.9: Transfer Function: 1 cladding

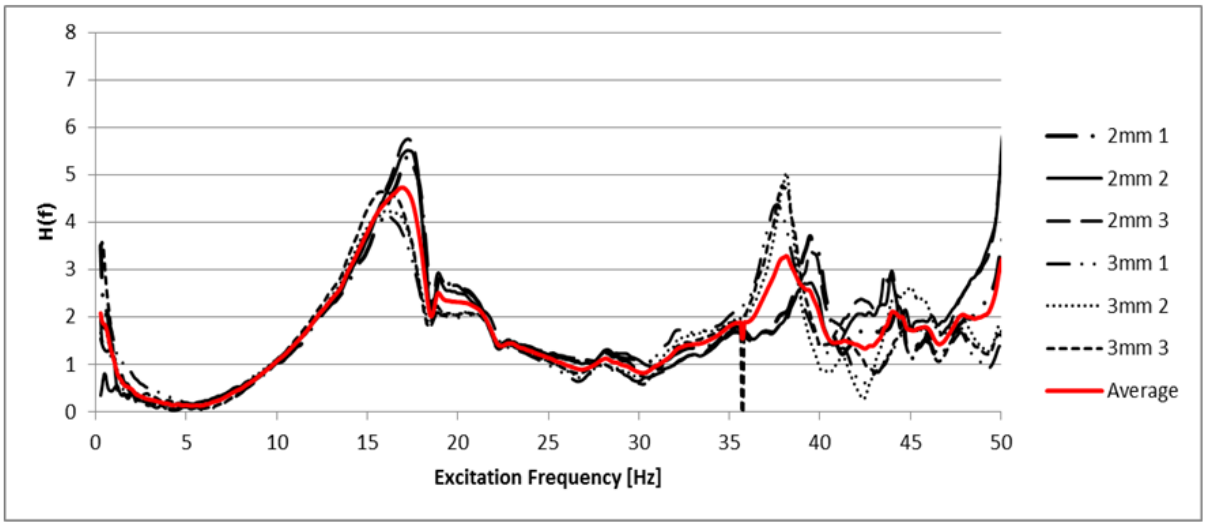

Figure 5.10: Transfer Function: 4 Cladding

When dealing with experimental data some methods to smooth the results can be used allowing an analysis of the overall trend of the studied parameter. For the study of the transfer function a weighted mobile mean method was used, having as bases an interval of 5 values. With this reasoning, parameter A_i at frequency $f = f_i$ can be estimated as shown in expression 5.8.

$$A_i = \frac{A_{i-2} + 2A_{i-1} + 4A_i + 2A_{i+1} + A_{i+2}}{10} \tag{5.8}$$

This method was applied to both the Power Spectral Density functions obtained through the dynamic analysis as well as to the Transfer Function obtained through these smoothed data.

5.2.1 Natural Frequency

Through the frequency response function it is possible to estimate the natural frequency of the system. This results can be compared with the ones obtained from CSTB (2016) using the Fourier Transform. Table 5.3 shows these results.

Table 5.3: Computed Natural Frequency of the System

Test	**Eigen Frequency [Hz]**	
	CSTB	**Frequency Response Function**
C1_b1	29.3	27.7
C4_b1	16.8	16.6
M1_b1	31.8	31.1
M4_b1	30.7	16.4
M1_b2	19.3	29.7
M4_b2	18.7	17.9

It can be observed in the previous table that the main influence on the natural frequency of the system

is related to the increase of its mass. In fact, when analysing the results for both one and four cladding systems, it is possible to observe that the change on the supporting wall material does not represent a considerable change on the system's natural frequency.

Some remarks should also be made about test M4_b1 and M1_b2 being the results attained through the frequency response function not entirely coherent with the ones obtained from CSTB's Fourier Transform analysis. While for the later this value is in agreement with the analysis performed by Politecnico di Milano, 2016 a more detailed study should be made for the first case.

For the 1 cladding in masonry wall with commercial brackets test the transfer function represented a natural frequency close to 30 Hz while the Fourier Transform showed a peak value at a frequency close to 20 Hz. As an example the Fourier Transform obtained from the first 2mm shock test is shown in figure 5.11.

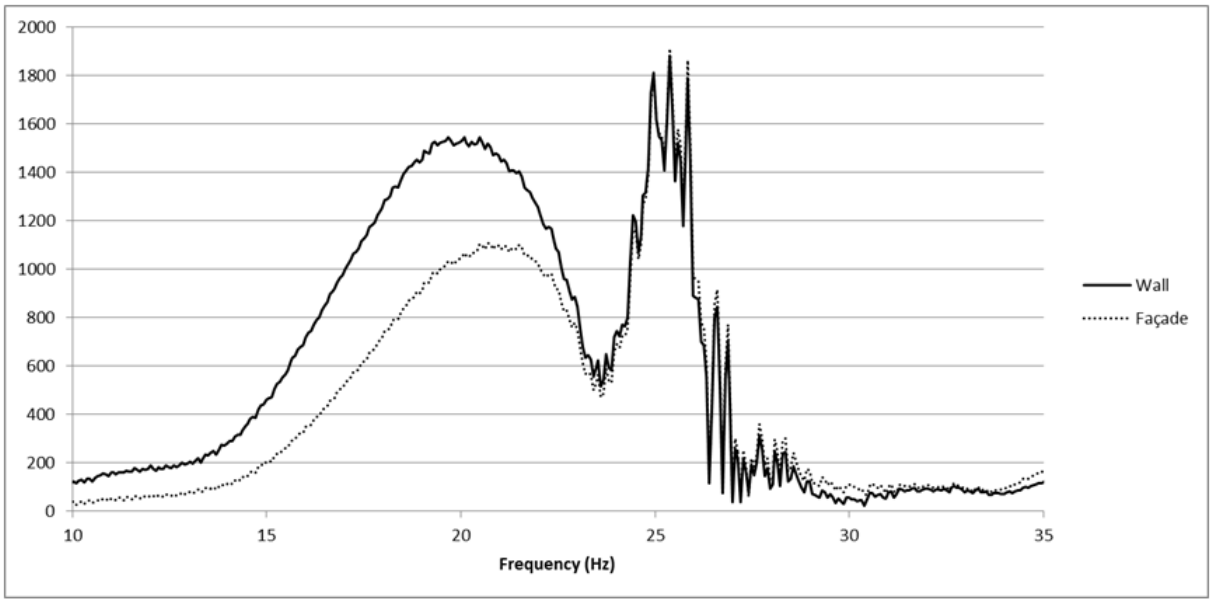

Figure 5.11: M1_b2 - Fourier Transform from 2 mm shock test

It can be observed a peak value for the façade's Fourier transform around 20 Hz, however, when compared with the Fourier transform of the supporting wall it can be seen that there is no amplification of façade's response. In other words, this peak can be related to a vibration mode belonging to the supporting wall that was not filtered by the non-structural element. Consequently, when dealing with the cladding system, the considered eigen frequency should be the one computed through the transfer function attained from the shock tests. Note that the results obtained through this function are more coherent with the estimated eigen frequencies for the other tests.

5.2.2 Amplification Factor

A plot of the amplitude of a response quantity as a function of the excitation frequency is called a frequency response curve. Hence, the previous plotted transfer function can be seen as a frequency response function of acceleration. Has a result, once known the transfer function for the system, an estimation of the amplification factor can be made.

Moreover, as stated before, it is possible to relate the peak amplification factor of a system with its damping ratio. Expression 2.18 gives the relation between these two parameters. This statement is valid for the maximum value of amplification, when the system is on a resonant state and for the structure's first mode of vibration, in other words for the first peak of the transfer function.

With this in mind it is possible to compute a theoretical value of amplification (α) based on the experimental value for damping obtained on the shock tests. These results can be compared with the experimental amplification computed through the experimental acceleration frequency response curve. The peak values attained for the first mode of the system shown in figure 5.9 can be analysed on table 5.4 while the results attained for this peak amplification analysis can be seen in table 5.5.

Table 5.4: Peak Values for the First Mode of the Transfer Function

Test	Peak Values	2mm			3mm			Average	
		1	2	3	1	2	3	Geomet.	Function
C1_b1	f1 [Hz]	28.25	27.68	27.73	25.68	27.29	27.29	**27.32**	**27.68**
	α	12.07	24.74	23.18	11.97	12.49	11.19	**15.94**	**13.48**
C4_b1	f1 [Hz]	17.30	17.23	17.23	15.88	15.81	15.74	**16.53**	**16.62**
	α	5.42	5.52	5.76	4.18	4.24	4.64	**4.96**	**4.73**
M1_b2	f1 [Hz]	29.99	39.96	29.72	29.24	30.60	30.19	**31.62**	**29.65**
	α	3.34	2.58	2.26	2.10	2.79	1.58	**2.44**	**2.71**
M4_b2	f1 [Hz]	19.34	20.63	19.61	18.25	18.12	18.12	**19.01**	**17.85**
	α	4.98	9.84	10.94	7.61	10.51	10.51	**9.07**	**6.10**

Table 5.5: Theoretical and Empiric Amplification Factors

Test			ζ	α_{max}		$\Delta\alpha$
			Damping Ratio	Theoretical (Chopra (1995))	Experimental (H(f))	
Concrete	**Ideal**	**1**	0.067	7.47	13.48	+ 81%
	Bracket	**4**	0.077	6.49	4.73	- 27%
Masonry	**Ideal**	**1**	0.028	18.08	17.92	- 1%
	Bracket	**4**	0.042	11.89	8.55	- 28%
	Simpson	**1**	0.035	14.37	2.71	- 81%
	Bracket	**4**	0.047	10.75	6.10	- 43%

Note that the results have some discrepancy between theoretical and experimental estimations. The fact that the peak amplification is extremely sensitive to damping ratio may result in some empirical errors. Figure 5.12 shows that even a small error on the estimation of the damping coefficient may lead to a significant error on the amplification factor.

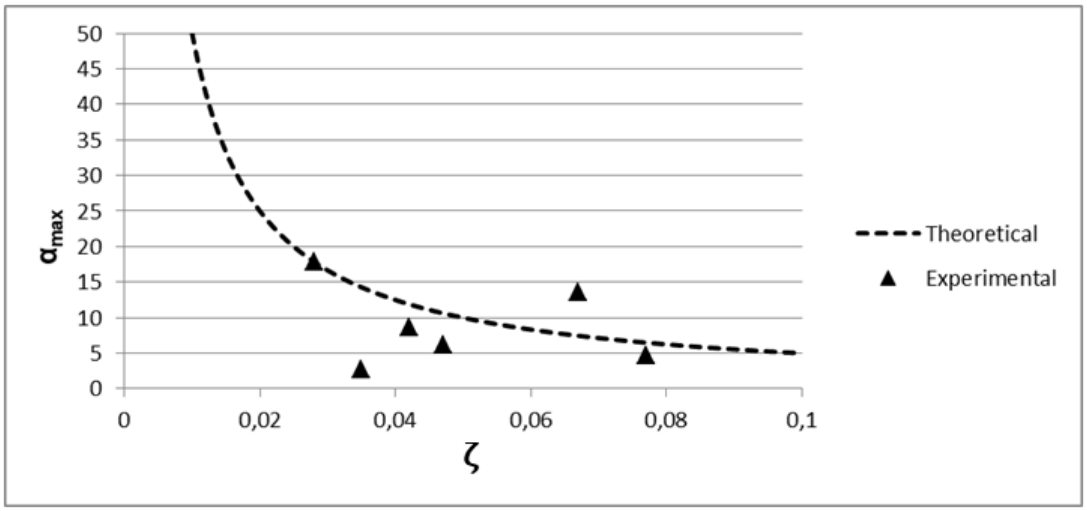

Figure 5.12: Relation between Damping Ratio and Maximum Amplification

Moreover, the fact that the logarithmic decrement is sensitive to the choice of points on bases of which it is computed makes this analysis less efficient. Furthermore, some small noises in experimental data are to be expected. Table 5.6 is an example on the different damping factors obtained for the 2 mm shock test on masonry wall with one cladding and ideal steel brackets. It can be seen that depending on the number of cycles considered there are significant differences on the damping factor and consequently large disparity on the estimated peak amplification, furthermore, a comparison between the theoretical values and the experimental ones can be made.

Table 5.6: Sensitivity of the Amplification Factor to the Number of Cycles

Number of Cycles	Damping Ratio	Maximum Amplification
1	0.020	25.6
2	0.039	12.9
3	0.037	13.6
4	0.034	14.6
5	0.030	16.4
6	0.028	17.8
7	0.024	20.7

It is clear from the previous results that this analysis was not effective. The experimental estimation of the damping factor may not be reliable for the evaluation of the amplification factor due to the very high scatter of results. Moreover, also the estimation of the peak amplification through the transfer function can have some errors. Nonetheless, it is important to notice that tests with higher mass lead, in general, to more consistent results. This may be related to the fact that the dynamic test is performed up to frequencies that are relatively close to the resonant state studied in this analysis. Consequently, a much lower range of frequencies is extrapolated when computing the transfer function.

5.3 Non-linear Behaviour

Until this section all computations made for the dynamic analysis assumed a linear behaviour of the system. In this way it is assumed that the results obtained from shock tests would characterize the structure throughout all dynamic phases. However, because the tests are performed with low and high acceleration, it is important to understand how this change in excitation may influence the system's response.

Accordingly, low acceleration (phase 1 and 2) and high acceleration (phase 7 and 8) were studied. In order to assert the systems behaviour, transfer functions were computed for these phases, analogously to the ones calculated for the shock tests, and the natural frequency of the system was estimated. The results can be seen in table 5.7.

Table 5.7: System's response to low and high acceleration

		1 Cladding				**4 Cladding**			
Phase		**1**	**2**	**7**	**8**	**1**	**2**	**7**	**8**
a [m/s^2]		**3.5**	**5.0**	**14.0**	**16.5**	**3.5**	**5.0**	**14.0**	**16.5**
C_b1	f1 [Hz]	29.0	28.6	27.3	27.7	**16.4**	**16.3**	**11.7**	**12.0**
	α (f1)	21.1	16.0	12.2	11.8	9.2	7.7	4.3	4.9
M_b2	f1 [Hz]	32.0	37.7	29.7	31.1	18.0	20.0	18.8	19.7
	α (f1)	1.8	1.4	3.9	2.3	13.2	7.1	8.9	7.4

It is possible to observe a decrease in the system's natural frequency for high acceleration tests for test in concrete with four cladding. This decrease is clear in figure 5.13 where the transfer functions for low and high acceleration are plotted. Since mass is constant, this change can be related with a decrease in the structure's stiffness. This change in stiffness depending on the loading characteristics indicates a non-linear behaviour of part or the whole system.

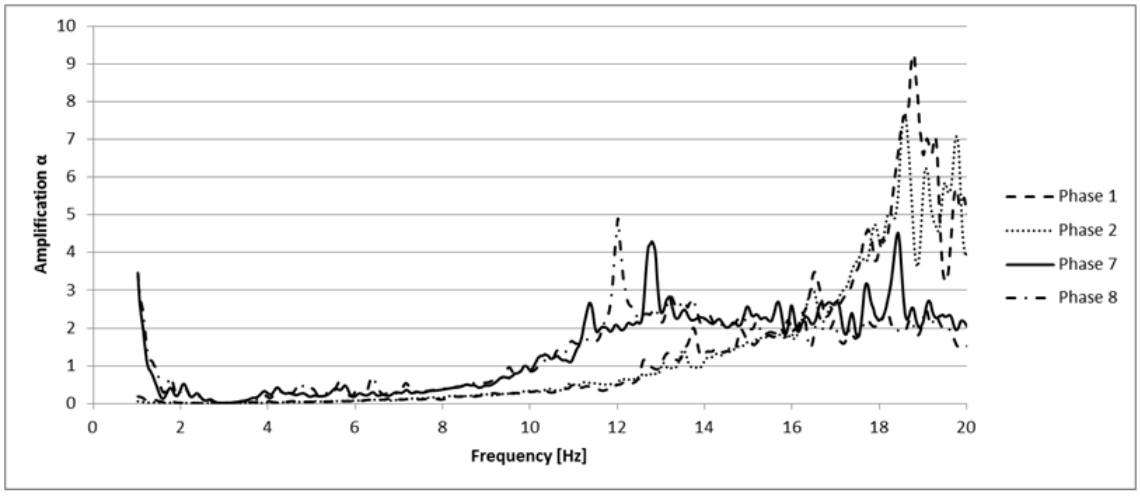

Figure 5.13: Transfer function for low and high accelerations - Test on Concrete Wall with 4 Cladding and Ideal Brackets

As it was previously mentioned, throughout the experimental test with four cladding on concrete wall a decrease of stiffness took place for high acceleration phases, causing a reduction of the natural frequency of the system. Two main aspects could cause the non-linearity on the system's behaviour: the fastener or the angle bracket. It was proven at the beginning of this dynamic analysis that the change of fastener's stiffness on the range of scope for this study had a negligible effect on the eigen frequency, consequently the behaviour of the bracket for this test was inspected.

Because the real load-displacement behaviour of the bracket is known, through CSTB's bending test, it can be checked if the accelerations from the dynamic test caused any non-linearity of this element. These computations can be done for the resonant phase, Phase 6, since it is at this phase that the non-linear behaviour is shown.

From the measured forces on fasteners it is possible to estimate the force acting on the bracket, equivalent to the one tested in the bending tests, from a simplified equilibrium equation. Figure 5.14 presents the quantities used on the definition of the equilibrium expression, where F_{fast} is the measured force on the fastener and F_{test} is the force to be compared with the results from the bending test.

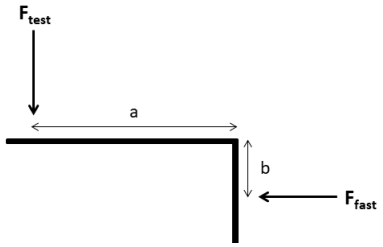

Figure 5.14: Estimation of Forces on the Bracket

The force on the bracket flange can be estimated as equation 5.9.

$$F_{test} = F_{fast}\frac{b}{a} \tag{5.9}$$

The results for the maximum forces on the fasteners during phase 6 of the four cladding test in concrete can be seen in appendix.

The forces acting on the four angle brackets are proportional to the forces measured on the fasteners, consequently the bracket with the higher load is the one associated to fastener 1. At this point it is important to recollect the results from the bending tests on steel brackets, namely the ones performed on the ideal bracket. It can be seen that the range of expected forces acting on the bracket are close to the yielding plateau, as represented appendix.

According to the previous results some of the brackets were no longer on their linear elastic range, in other words, the initial stiffness no longer characterizes these elements. It is clear from the previous plot that the real stiffness throughout this phase is lower than the initial tangent stiffness. This result is in agreement with the lower natural frequencies obtained for the higher acceleration phases.

According to the post-dynamic tests, no decrease of stiffness was observed in this test, this can be related with the previous results assuming that even though the bracket left its linear elastic range it did not reached the yielding plateau, no failure occur, the bracket sustained a non-linear elastic behaviour.

5.4 Resonant State

When analysing the test results on the concrete shaking wall it is possible to observe that a higher load on fasteners is attained in phase 6 for four cladding test. This result is in agreement with the previous remarks made about the non-linearity of the system. In fact, when computing the eigen frequencies for higher accelerations it is possible to observe that this value is close to 12 Hz.

To this matter a closer study of phase 6 under 13 Hz frequency can be done (figure 5.15), since it can be observed that the system is close to the resonant state during this stage of the test. Hence, a transfer function for this phase can be obtained allowing the study of the façade's relative acceleration amplification factor.

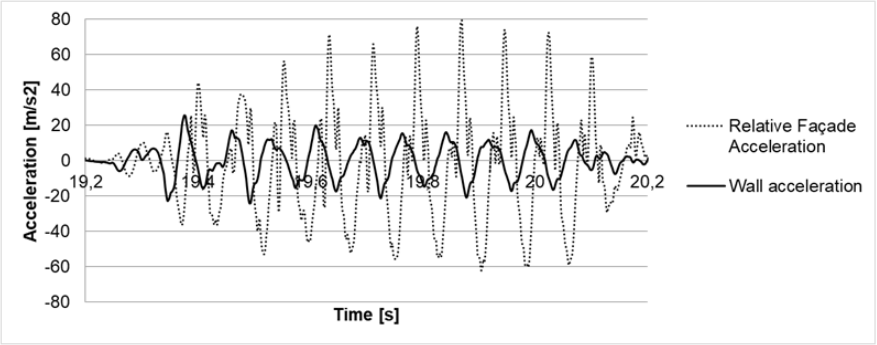

Figure 5.15: Experimental Acceleration for Phase 6 - 13 Hz

It is possible to notice on plot 5.16 that the transfer function has a peak for an acting frequency of around 12 Hz with an amplification factor of $\alpha_{max} = 5.30$.

These theoretical results can be compared with the experimental results. It is possible to estimate the experimental amplification simply as the ratio between the relative acceleration on the façade and the one on the wall. If these computations are performed, with the previously plotted results for this phase, it is possible to estimate an amplification of $\alpha_{experimental} = 5.26$, obtained as the average of the computed amplification for each cycle. Thus, it is possible to understand that a resonant state was reached with a maximum amplification close to the one estimated through the transfer function.

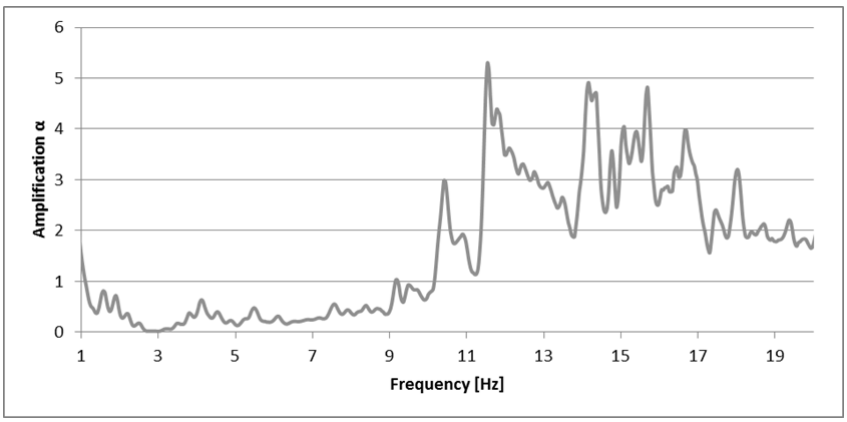

Figure 5.16: Transfer function for Phase 6 - 4 claddings

5.4.1 Comparison with the Code

It is possible to compare the values obtained experimentally with the ones prescribed by the codes. CSTB prescribes a constant amplification factor of 2.75 while the amplification prescribed by EC8 is dependent on the ratio between the eigen frequency of the element and the acting frequency. In order to compare the code with the theoretical amplification an expression of the type 5.10 is seek.

$$F = \alpha \times m a_g \tag{5.10}$$

where

F is the equivalente seismic force;

m is the mass of the non-structural element;

a_g is the ground acceleration;

α is the equivalent amplification factor between the ground acceleration and the relative acceleration on the non-structural element.

In this way it is possible to rewrite Eurocode 8 expression CEN (2014) with the following coefficients, a local amplification factor considering the frequency dependency, A_{EC8} (expression 5.11), and a global amplification factor that has into consideration the location of the element, G_{EC8} (equation 5.12).

$$A_{EC8} = \frac{3}{1 + \left(1 - \frac{f_1}{f_a}\right)^2} \tag{5.11}$$

$$G_{EC8} = \left(1 + \frac{Z_a}{H}\right) A_{EC8} - 0.5 \tag{5.12}$$

where

f_1 is the frequency of the action on the structure, in this case, the maximum frequency on each phase;

f_a is the eigen frequency of the façade system, in this case, coming from shock tests;

$\frac{Z_a}{H}$ is the ratio between the height of the non-structural element and the total height of the structural, equal to one for the considered dynamic test.

Hence, considering expression 2.20 the equivalent amplification factor in Eurocode 8 can be written as seen in expression 5.13.

$$\alpha_{EC8} = \frac{1}{q_a} G_{EC8} = \frac{1}{q_a} \left(2 A_{EC8} - 0.5\right) \tag{5.13}$$

In the case that is being studied, different values are obtained for the amplification factor depending on the behaviour factor considered for the system. For the prescribed behaviour factor for cladding systems, $q_a = 2$, a maximum amplification factor of $\alpha_{max} = 2.75$ is attained. This coincides with the value prescribed by CSTB. However if a unit behaviour factor is considered $\alpha_{max} = 5.5$ the maximum value attainable through this formulation.

As stated before Sullivan, Calvi, and Nascimbene (2013) estimates an amplification factor for the acceleration acting on the non-structural element as expressed in equation 2.19. This formulation has into consideration not only the relation between the acting frequency and eigen frequency of the element, but also considers the damping coefficient of the system. Being this coefficient estimated through the shock tests it is possible to compare the attained transfer function to the theoretical value estimated by Sullivan.

With the previous considerations in mind it is possible to relate the amplification obtained through the computation of a transfer function with the one prescribed by the code. The results can be seen on figure 5.17 and 5.18, for tests in concrete for both 1 and 4 cladding.

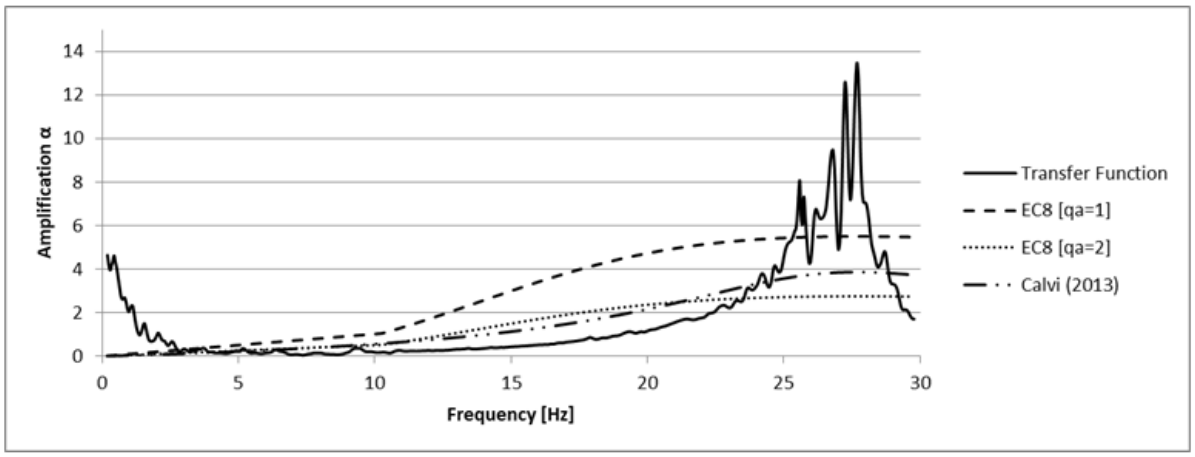

Figure 5.17: Amplification Factor: Comparison between testing and Eurocode - 1 cladding

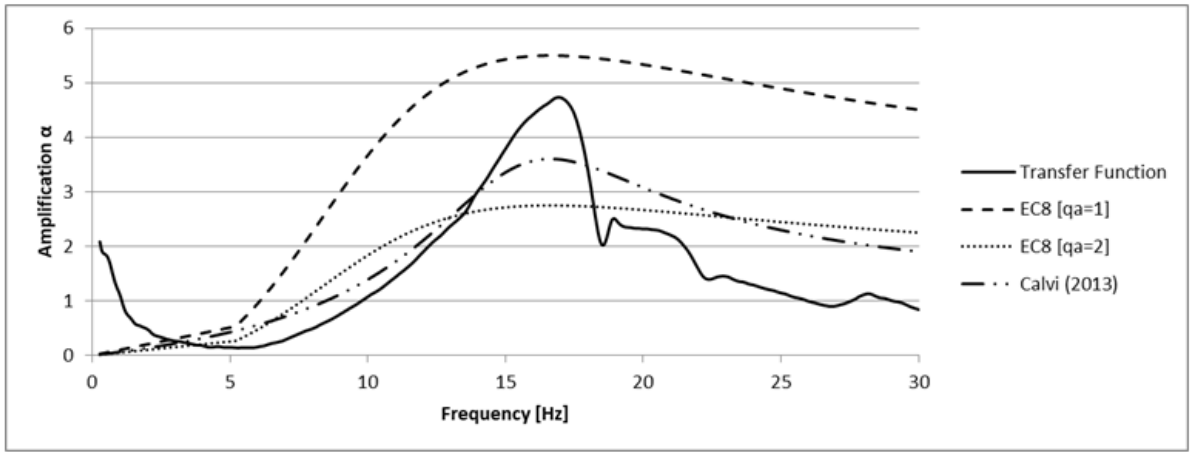

Figure 5.18: Amplification Factor: Comparison between testing and Eurocode - 4 cladding

It can be seen that the code prescribed magnification of the action is always on the safe side unless it is close to the resonant frequency of the element. This analysis is particularly interesting for the higher mass system with lower natural frequency. As expected it can be observed in the previous plot, if design is made considering a linear behaviour of the structure an overestimation of the amplification is obtained, however the prescribed behaviour factor may underestimate the action on the element if the acting frequency is close to the resonant frequency.

Additionally, it can be observed that Sullivan, Calvi, and Nascimbene (2013) estimation is a middle ground between the two limit cases proposed by Eurocode 8. This means that this formulation provides for the resonant state a more conservative approach than the one prescribed by Eurocode 8. However, a final remark should be made to the fact that, this expression is dependent on the damping coefficient, which, as stated before, may be difficult to accurately estimate in a real system. In other words, the expression suggested by these authors may be difficult to use in a practical basis.

Furthermore, it is possible to estimate the relation between the system's natural frequency and a maximum value, for which the code's amplification intersects the transfer function. These values are presented in table 5.8, where f represents the intersection between the two amplification curves.

Table 5.8: Intersection between EC8 and Frequency Response Function

Number of Cladding	**f1 [Hz]**	**f [Hz]**	**f/f1**
1	27.7	23.5	85%
4	16.6	13.5	81%

Being the resonant state reached in the four cladding test, it might be of interest to understand if the forces estimated by EC8, considering the two limit behaviour factors, are on the safe side when compared to the experimental forces on fasteners. The results can be seen in appendix.

As a remark it is important to notice that the results for the behaviour factor equal to two have the same amplification as the one considered by CSTB, however if CSTB's prescription is considered, than the existence of a group of anchors is taken into account through the redistribution factors K_{alea} and the R_a. Note that the maximum redistribution is 55%, which if this factors are considered is close to the theoretical prediction.

In the previous results it was assumed the expressions used previously for the estimation of loads on fasteners, namely equation 4.1. Moreover it was hypothesised that the equivalent force is equally distributed among the fasteners, and the real acceleration of the wall was considered. An average acceleration of 14.1 m/s^2 was computed, slightly higher than the 11.2 m/s^2 prescribed for this phase. Moreover, the previous results can be seen in plot 5.19, where the relation between theoretical predictions and experimental results is displayed.

It would be expected that the forces on the fasteners, arising from the higher behaviour factor, to be underestimated. However, in the present case, an average overestimation of forces of 20% error was found. While computation method for both Eurocode 8 with an unit behaviour factor and through the experimental transfer function largely overestimate the forces acting on the anchor. However, it can be seen from the results for the 1 cladding system that on a resonant state this is not always valid. In fact, there are some circumstances, such as higher accelerations, less damped systems or lower mass systems, where the behaviour factor prescribed for façade systems may not be on the safe side. Hence, a behaviour factor of $q_a = 1.5$ may be more suitable for situations where resonance is to be expected.

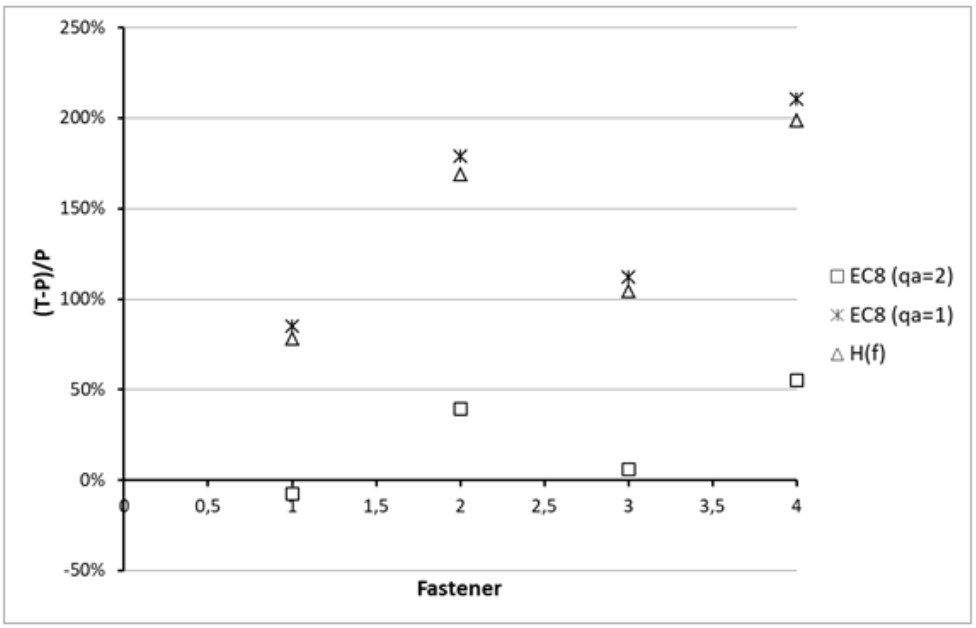

Figure 5.19: Comparison between theoretical and experimental forces on fasteners

Chapter 6

Higher Vibrations Modes

6.1 Simplified Model

Before this section, only the first vibration mode of the system was studied. However, in order to better understand the behaviour of the system a simplified dynamic model was build to consider also out of plane vibrations. The model was built as a three degree of freedom system, based on the previously explained model allowing out of plane motion, as shown in figure 6.1.

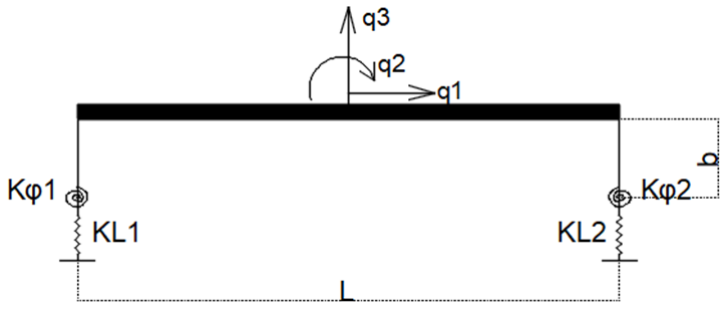

Figure 6.1: Simplified three degrees of freedom model

The influence of the anchoring system is portrait as a combination of a linear and rotational spring at the base of the angle brackets. Once again, the fact that the fasteners may have different properties is taken into account. With this is mind, the mass and stiffness matrix of the system may be defined as expressions 6.1 and 6.2, respectively.

$$[M] = m_t \begin{bmatrix} 1 & 0 & 0 \\ 0 & \frac{L^2}{6} & 0 \\ 0 & 0 & 1 \end{bmatrix} \tag{6.1}$$

$$[K] = \begin{bmatrix} \frac{12EI}{b^3}\left(\frac{1+\eta_1}{1+4\eta_1}+\frac{1+\eta_2}{1+4\eta_2}\right) & \frac{-6EI}{b^2}\left(\frac{1+2\eta_1}{1+4\eta_1}+\frac{1+2\eta_2}{1+4\eta_2}\right) & 0 \\ " & \frac{4EI}{b}\left(\frac{1+3\eta_1}{1+4\eta_1}+\frac{1+3\eta_2}{1+4\eta_2}\right)+\frac{L^2}{4}\left(k_{L2}-k_{L1}\right) & \frac{L}{2}\left(k_{L2}-k_{L1}\right) \\ " & " & k_{L1}+k_{L2} \end{bmatrix} \tag{6.2}$$

$$with, \eta_i = \frac{EI}{bk_{\varphi_i}} \tag{6.3}$$

6.2 Eigen Frequency

Because the transfer function was estimated for all the test layouts, it is possible to estimate the eigen frequency for the second vibration mode, these values are summarized on table 6.1. The transfer functions used to estimate these values are presented in appendix.

Table 6.1: Transfer Function - Eigen Frequency [Hz]

Test	$\mathbf{1^{st}Mode}$	$\mathbf{2^{nd}Mode}$
C1_b1	27.7	37.7
C4_b1	16.6	37.9
M1_b1	31.1	38.1
M4_b1	16.4	27.3
M1_b2	29.7	47.0
M4_b2	17.9	30.5

6.3 Model Calibration

A modal analysis was performed, to this sense, the eigen values and eigen vectors of the system were computed. It was possible to observe from the first computations that, if both fasteners have the same stiffness, the second mode of vibration is linked with the third degree of freedom, however, from experimental testing it was possible to observe that fastener pull out was related with the torsional displacement. Additionally, the residual tests on fasteners showed that the stiffness was not equal for both anchors, and therefore, it is important to understand the consequences of this uncertainty on the higher vibration modes.

Moreover, it can be seen that, even tough the fastener stiffness does not represent a significant influence on the natural frequency of the system, it clearly influences its second eigen frequency.

The first model iteration showed that following the reasoning used for the one degree of freedom a big overestimation of the stiffness was attained. To this sense it was important to understand the interaction between the bracket and the fastener. The simplified model represented in figure 6.2 was used and the

total linear stiffness estimated as a combination from the bracket and the fastener stiffness as shown in equation 6.4.

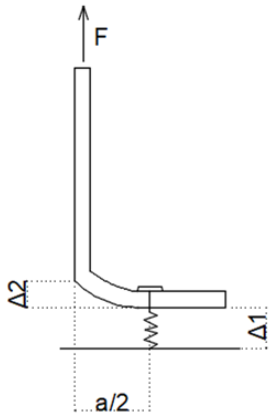

Figure 6.2: Model's equivalent axial stiffness

$$K_{Li_{equivalent}} = \frac{1}{\frac{1}{K_{Li}} + \frac{1}{K_b}} \tag{6.4}$$

where,

K_{Li} =axial stiffness of the fastener;

K_b =bending stiffness of the bracket.

If the axial stiffness of the fastener can be directly estimated from the static tests, the bracket stiffness needs to be indirectly estimated. From the bending tests it is possible to compute the value for the bracket characteristic EI. Based on this parameter, two different limit situation may occur: double-clamped or clamped-hinged scheme, depending on the interaction between the fastener and the bracket, as shown in figure 6.3, where L is taken as half of the bracket flange length.

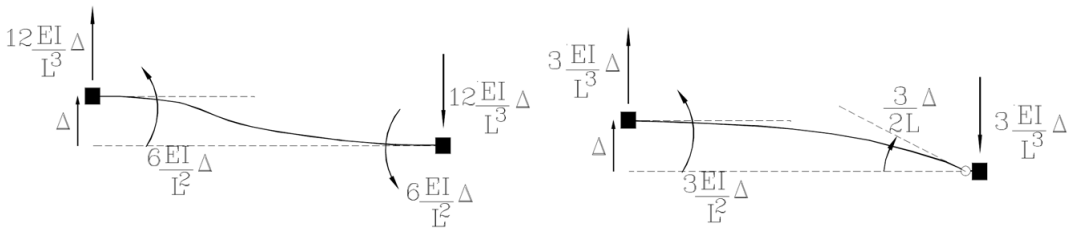

(a) double-clamped (b) clamped-hinged

Figure 6.3: Bracket stiffness estimation - limit cases

These two limit situations can be represented by two different stiffness values, as shown in the previous scheme (figure 6.3). When analysing the natural frequency of the structure it was possible to observe that the results concerning the clamped-hinged scheme were underestimating this parameter when compared with the experimental values. To this sense a mean value between these two limits was assumed. This estimation showed that for the first mode, the results from the three degree of freedom model were similar to the results obtained for the simplified single degree of freedom model.

With the previous reasoning it is assumed that the fastener will partially constrain the rotation of the

bracket. Obviously, in the real behaviour of the system, bracket rotation exists, however, is it assumed that this movement is already portrait with the rotational spring and is not significant when analysing the in-plane translation of the façade system. This is coherent with the fact that the fictional rotational spring has a stiffness considerably lower that the steel bracket.

With this in mind, it is possible to attain the following results for the eigen frequency associated with the second mode of vibration. The comparison between experimentally estimated and predicted eigen frequency by the model can be seen in table 6.2.

Table 6.2: Second mode eigen frequency [Hz]

Test	Transfer Function	Model Estimation
C1_b1	37.7	70.7
C4_b1	37.9	40.9
M1_b1	38.1	67.9
M4_b1	27.3	39.3
M1_b2	47.0	106.6
M4_b2	30.5	60.7

It is possible to see that the estimated frequency is higher than the one predicted by the transfer function, however, these results were obtained assuming an equal distribution of forces on the fasteners. To this sense it is possible to estimate the ratio between the stiffness of the two fasteners for each test layout. This estimation can be seen in table 6.3.

Table 6.3: Stiffness ratio estimation

Test	Transfer Function [Hz]	$\frac{k_{L2}}{k_{L1}}$	Model Estimation [Hz]
C1_b1	37.7	0.25	39.0
C4_b1	37.9	0.70	38.0
M1_b1	38.1	0.25	37.5
M4_b1	27.3	0.40	27.1
M1_b2	47.0	0.15	45.2
M4_b2	30.5	0.20	29.7

When analysing the eigen vectors of the system with the estimated redistribution, it is clear that the second vibration mode is represented by a combination of torsion and out-of-plane displacement, as expected from the failure observed during tests on concrete wall with ideal brackets and a 4 cladding system. However, an overestimation of the redistribution is performed. In other words, this model is still overestimating the system's stiffness. In fact, it was shown previously that the stiffness ratio between the two horizontal fasteners is within the computed range of 0.65 which is coherent with the results obtained from the experimental tests that show a redistribution within the upper and lower 50% limit. It is important, nonetheless, to note the fact that this model shows the importance of the redistribution on the higher vibration modes.

Chapter 7

Conclusion

Throughout this study the dynamic analysis of a façade cladding system was performed. The results from the experimental data were compared with both the results from simple dynamic models as well as with some European codes, namely Eurocode 8 and a prescription made by CSTB specifically for this type of systems. Due to this comparison it was possible to reach some conclusions related to the behaviour of façade anchor systems under simulated seismic action.

Initially a simple study was executed relating the forces acting on the fasteners with both CSTB and Eurocode 8 predictions. It was possible to observe that using a constant amplification factor may underestimate the forces acting on the fasteners, in this sense, the dependence of the seismic force acting on the cladding from the relation between the acting frequency and the natural frequency of the system is relevant and should be taken into consideration when designing a façade system.

As stated, Eurocode 8 provides a low boundary estimation for the force acting on the façade system. The results from the previous analysis may indicate that this lower boundary might not always be on the safe side. In other words, the prescribed behaviour factor for façade elements, a behaviour factor equal to two, might lead to an underestimation of the seismic force, particularly, when the structure is near its resonant state. Hence, for systems where resonance can be expected a 1.5 behaviour factor of may be more advisable.

Moreover, it is essential to distinguish between the behaviour of fasteners working as a group and the one from a single fastener. In fact, the performed analysis showed that there is some redistribution of forces through the fasteners and that indeed, there is some uncertainty on the distribution of forces on these elements. Concerning this uncertainty, from the results attained, it is possible to reach 1.5 as an acceptable factor to take this phenomenon into consideration. Actually, the parameter proposed by CSTB, that considers a 50% redistribution, represents the scatter of forces acting on the fasteners successfully, even after entering a non-linear behaviour of the system through yielding of the supporting brackets.

If this unpredictability of distribution of forces is obtained in a controlled environment such as a research laboratory, in practical cases, installation of anchors to support a system of this kind may lead to a more pronounced difference on the forces acting on the fasteners. To this sense it was predicted

a limit ratio for the stiffness of two conjugated fasteners, for which the prescribed 1.5 factor is valid. It was deduced that, if the stiffness ration between two fasteners is higher than 65% then the prescribed redistribution factor provides a safe estimate of the force's redistribution.

As stated before, the natural frequency of the system has a significant influence on the acceleration amplification of the cladding and consequently on the actions to which it and its anchoring system are subjected. In this sense, it is of interest to study the influence of the loss of stiffness on this parameter. It was shown that for the range in which the 1.5 redistribution factor is valid, the rearrangement of supporting reactions on the anchors does not influence significantly the natural frequency of the structure. In other words, even though distinct stiffness parameters have a considerable influence on the forces acting on the fastener, the overall stiffness is not significantly affected by it. This means that, even with a unpredictable redistribution of forces, it is possible to estimate the overall behaviour of the system.

This apparent range in which the stiffness of the fasteners has a small influence on the structure's eigen frequency is sustained by the analysis performed with the residual stiffness of the anchors after the dynamic test on a framed wall. In reality, even though there is a considerable decrease on the stiffness of these elements, its influence on the system's natural frequency is negligible for the range in which the test was performed. In fact, it was shown that this parameter is dependent on the relation between the bracket's and fastener's stiffness and for ratios going from zero until 60% the decrease in natural frequency is lower than 0.1%.

A special remark can be made to how, in a practical sense, analytic models may not be viable. This has to do mainly with the fact that some parameters are extremely hard to accurately estimate through experimental data. To this matter a study on the sensitivity of the damping ratio was made and it was shown that, combined with the difficulty in correctly assess this parameter, small errors on its computation can lead to high errors on the estimation of the amplification factor. With this is mind, theoretical expressions, such as the one proposed by Sullivan, Calvi, and Nascimbene (2013), that depend on this parameter may be difficult to use.

Furthermore, code prescription not only for equivalent seismic force but also for the estimation of the forces acting on the fasteners may be useful. Considerations such as the redistribution of forces can lead to a safer design for these elements. Additionally, the behaviour of anchors under seismic loading is still to be further developed. European anchor qualifications deal with the assessment of metal anchors on concrete under seismic load, however, evaluation on different base materials may be of importance. Furthermore, the evaluation of façade systems is not contemplated on the code, an so, this project may be seen as starting point for a future technical approval of these anchoring systems.

The previous results show that, generally, the design of the studied façade cladding systems can be done independently from the choice of the fasteners. In the same way, the assessment of fasteners' behaviour can be done simply with single fastener testing. In fact, when designing the system's anchorage system two paths can be followed. If the design is meant to protect the fasteners, then the prediction of forces acting on the anchorage system can be obtained simply by considering the resisting moment of the angle brackets. On the other hand, if the systems intent is to protect the angle brackets, the forces on the fasteners can be estimated through European codes. Nonetheless, in this case, for systems where

resonance can be expected, the lower boundary assuming a behaviour factor of 2 may not be on the safe side. In other words, for these situations a factor of 1.5 may be more advisable.

As a final remark, simplified dynamic models may be helpful to evaluate the behaviour of façade cladding systems and, as shown in the previous analysis, may lead to acceptable results for an initial estimation of parameters, such as the natural frequency. However, considering the safety and economical importance of non-structural elements a deeper study should be made. If the seismic design of structures has improved largely in the past years, the uncertainties on the behaviour of non-structural elements is still significant. It may be important in the future to expand the study of these elements leading, for example, to more detailed and practical prescriptions in European codes, not only for their design, but also for the design of their anchoring systems.

Bibliography

Abdel-Mooty, Mohamed, Nasser Zaki Ahmed, and Eman Mahmoud (2015). “Seismic Analysis of Non-structural Elements in Buildings Considering Different Codes”. In: *International Journal of Civil and Structural Engineering* 2.2.

Calvi, Paolo Martino (2014). “Relative Displacement Floor Spectra for Seismic Design of Non Structural Elements”. In: *Journal of Earthquake Engineering* 18.7, pp. 1037–1059.

CEN (2014). *Eurocode 8: Design of structures for earthquake resistance-Part 1: General rules, seismic actions and rules for buildings*.

Chopra, Anil K et al. (1995). *Dynamics of structures*. Vol. 3. Prentice Hall New Jersey.

Clough, Ray W and Joseph Penzien (1975). *Dynamics of Structures*. McGraw-Hill International Book Company.

CSTB (2013). “Stabilite en zones sismiques - Systemes de bardages rapportes faisant lobjet dun Avis Technique”. In: Centre Scientifique et Technique du Bâtiment - Cahier 3725.

— (2016). *Test Report MRF 16 26063696 on the behavior of the anchor in masonry under seismic loading*. Tech. rep. Centre Scientifique et Technique du Bâtiment.

Eligehausen, Rolf, Rainer Mallée, and John F Silva (2006). *Anchorage in concrete construction*. Vol. 10. John Wiley & Sons.

EOTA (2013a). *Technical Report 45 - Design of Metal Anchors for use in Concrete under Seismic Actions*.

EOTA, ETAG (2010). *No 020: Guideline for European Technical Approval of Plastic Anchors for Multiple Use in Concrete and Masonry for Non-Structural Applications, ANNEX C: Design Methods for Anchorages*.

— (2012). *No 020: Guideline for European Technical Approval of Plastic Anchors for Multiple Use in Concrete and Masonry for Non-Structural Applications, PART 1: General*.

— (2013b). *No 001: Guideline for European Technical Approval of Metal Anchors for Use in Concrete, Annex E: Assessment of Metal Anchors under Seismic Action*.

— (2013c). *No 001: Guideline for European Technical Approval of Metal Anchors for Use in Concrete, PART 1: Anchors in General*.

Filiatrault, Andre and Timothy Sullivan (2014). “Performance-based seismic design of nonstructural building components: The next frontier of earthquake engineering”. In: *Earthquake Engineering and Engineering Vibration* 13.1, pp. 17–46.

Fröhlich, T. et al. (2017). “Experimental Investigations on Seismic Behaviour of Post-Installed Anchorages in Nuclear Power Plants”. In: 16^{th} *World Conference on Earthquake (16WCEE 2017)*.

Hoehler, Matthew Stanton (2006). *Behavior and testing of fastenings to concrete for use in seismic applications*. Institut fr Werkstoffe im Bauwesen der Universitt Stuttgart.

Hoffmeister, B, M Gündel, and M Feldmann (2011). “Floor response spectra for dissipative steel supports of industrial equipment”. In: *COMPDYN 2011, III ECCOMAS Thematic conference on computational methods in structural dynamics and earthquake engineering, Corfu, Greece, 26–28 May 2011*.

IBC, ICC (2012). “International Code Council”. In: *International Building Code. International Code Council: Washington DC, United States*.

Izzi, Matteo et al. (2016). “Experimental investigations and design provisions of steel-to-timber joints with annular-ringed shank nails for Cross-Laminated Timber structures”. In: *Construction and Building Materials* 122, pp. 446–457.

Mahrenholtz, P and T Pregartner (2016). “Qualification and design of seismic anchors - Requirements in New Zealand and Australia”. In: *NZSEE Conference*.

Miranda, E and S Taghavi (2003). “Estimation of seismic demands on acceleration-sensitive nonstructural components in critical facilities”. In: *Proceedings of the Seminar on Seismic Design, Performance, and Retrofit of Nonstructural Components in Critical Facilities*, pp. 29–2.

Muciaccia, Giovanni (2017). “Behavior of Post-Installed Fastening under Seismic Action”. In: *ACI Structural Journal* 114.1, p. 75.

Politecnico di Milano (2016). *Plastic anchors for fixing façade claddings through angle brackets in masonry and concrete under seismic action. Phase 3 Report Background document for an EAD*. Tech. rep. Department of Civil and Environmental Engineering.

Salawdeh, Suhaib and Jamie Goggins (2016). “Seismic Design and Performance of Non-structural Elements”. In: *Civil Engineering Research in Ireland 2016 (CERI2016), At Galway, Ireland*.

Sullivan, Timothy J, Paolo M Calvi, and Roberto Nascimbene (2013). “Towards improved floor spectra estimates for seismic design”. In: *Earthquakes and Structures* 4.1, pp. 109–132.

Trespa (2012). *Material Property Datasheet - Trespa METEON*. Code U8001 version 3.2.

Vijayanarayanan, AR, Rupen Goswami, and CVR Murty (2012). “Determining Levels of Seismic Shaking Effects in Buildings for securing Non-Structural Elements”. In: *Fourth International Conference on Structural Stability and Dynamics (ICSSD 2012)*, pp. 4–6.

Appendix A

Confidentiality

The appendices presented in this work are confidential and will not be presented in the public thesis document.